2006

The Role of Electrospinning in the Emerging Field of Nanomedicine

S. Y. Chew
Johns Hopkins University

Y. Wen
University of Nebraska-Lincoln

Yuris A. Dzenis
University of Nebraska-Lincoln, ydzenis@unl.edu

K. W. Leong
Johns Hopkins University, kam.leong@duke.edu

Published in final edited form as:
Curr Pharm Des. 2006 ; 12(36): 4751–4770.

The Role of Electrospinning in the Emerging Field of Nanomedicine

SY Chew[1,2], **Y Wen**[3], **Y Dzenis**[3], and **KW Leong**[1,*]

1*Department of Biomedical Engineering, Johns Hopkins University, Baltimore, MD 21205*

2*Department of Materials Science and Engineering, Johns Hopkins University, Baltimore, MD 21205*

3*National Nanofiber Facility and Center for Materials Research and Analysis, Department of Engineering Mechanics, University of Nebraska-Lincoln, Lincoln, NE 68526-0588, USA*

Abstract

The fact that *in vivo* the extracellular matrix or substratum with which cells interact often includes topography at the nanoscale underscores the importance of investigating cell-substrate interactions and performing cell culture at the submicron scale. An important and exciting direction of research in nanomedicine would be to gain an understanding and exploit the cellular response to nanostructures. Electrospinning is a simple and versatile technique that can produce a macroporous scaffold comprising randomly oriented or aligned nanofibers. It can also accommodate the incorporation of drug delivery function into the fibrous scaffold. Endowed with both topographical and biochemical signals such electrospun nanofibrous scaffolds may provide an optimal microenvironment for the seeded cells. This review covers the analysis and control of the electrospinning process, and describes the types of electrospun fibers fabricated for biomedical applications such as drug delivery and tissue engineering.

1. Introduction

Nanomedicine profits from the innovative application of nanotechnology to medicine. An area of interest is to produce synthetic analogs of the extracellular matrix, which contains many nanoscale features. Such biomimetic nanostructures would have important implications in the basic studies of cell biology and in applications for regenerative medicine and medical device design. The nanoscale comes into the picture because *in vivo* the extracellular matrix or substratum with which cells interact often includes topography at the submicron scale. For example, the basement membrane that separates tissues such as epithelia, endothelia, muscle fibers, and the nervous system from connective tissue compartments possesses a complex mixture of pores, ridges, and fibers with sizes in the nanometer range [1,2]. The literature clearly indicates that cells respond to the nanotopography of synthetic substrates in terms of adhesion, proliferation, migration, and gene expression. An important and exciting direction of research in nanomedicine would be to gain a fundamental understanding of how cells respond to nanostructures. This would be best accomplished by conducting cell culture studies on well-defined nanostructures produced by techniques perfected for microelectronics industry, such as electron beam lithography, x-ray lithography, laser ablation, nano-embossing, and nanoimprinting. However, in parallel there is also a need to produce nanostructures by simple fabrication techniques for applications such as tissue engineering.

*Address correspondence to this author at the Department of Biomedical Engineering, Department of Materials Science and Engineering, Johns Hopkins University, Baltimore, MD 21205 and National Nanofiber Facility; E-mail: kam.leong@duke.edu.

Tissue engineering takes many forms. Most approaches involve a scaffold for cells to attach, differentiate, proliferate, and eventually develop into a tissue suitable for implantation. Alternatively the cells, particularly xenogenic or transformed cells, are encapsulated in a semipermeable membrane for immunoprotection and applied *in vivo* as part of a cell-based artificial organ, or *ex vivo* as an extracorporeal device. Artificial pancreas and artificial liver represent the latter examples. In all cases, a scaffold that can interact and influence the cellular behavior is a crucial component.

Fibrous scaffolds are attractive for tissue engineering because of their inherent advantages of high surface area for cell attachment, controlled porous architecture, and a 3-D microenvironment for cell-cell contact. Conventional fibers produced by mechanical fiber spinning usually measure tens of microns in diameter. Such fibers have relatively low specific surface area and their diameters are far larger than the diameters usually encountered in nature. Smaller, submicron-diameter polymeric fibers, or nanofibers, may provide stronger topographic cues by mimicking the filamentary ECM. Nanofibers composed of natural or biodegradable polymers can also be tailor-designed to possess the tissue-matching mechanical compliance. Unlike carbon nanotubes or other metallic nanorods, continuous polymeric nanofibers may also have reduced potential health hazards that are associated with discontinuous nanomaterials and nanoparticles [3,4]. Another advantage of electrospinning is the possibility of encapsulating drugs in the fibers. Optimal tissue engineering requires more than an inert scaffold to serve merely as a substrate for cell attachment and cell growth. Cues or signal molecules in the form of adhesion molecules, growth and differentiation factors, or even plasmid DNA, should be incorporated into these scaffolds in a spatially defined manner to orchestrate the growth of new tissue. Growth factors encapsulated in electrospun nanofibers constitute a biofunctional scaffold that may best mimic the ECM.

Until recently, there are no techniques that can manufacture nanofibers economically. Conventional mechanical fiber spinning cannot produce fibers with diameters smaller than 2 micrometers. Melt blowing produces non-woven mats of fibers with diameters around or slightly below a micrometer. However, these fibers tend to be discontinuous and highly non-uniform in diameter. An island-in-the-sea method based on mechanical spinning of polymer blends with subsequent removal of selected components produces fibers of micron or slightly submicron diameters [5]. This method is however very expensive. One technique that can consistently produce continuous polymeric nanofibers is electrospinning.

2. Electrospinning Process

2.1. Experimental Process Setup and Examples of Resulting Nanofibers

Electrospinning consists of spinning polymer solutions or melts in high electric fields. A schematic of the process is shown in Fig. 1. The process is based on the principle that strong electrical forces overcome weaker forces of surface tension in the charged polymer liquid. At certain threshold voltage, a fine charged jet is ejected from the tip of a capillary tube. Subsequently, the jet moves in the direction of the external electric field, elongates according to external and internal electrical forces, and experiences instabilities [6]. The jet segments are then deposited on a substrate in the form of random nonwoven mat of nanofibers. Over 200 synthetic and natural polymers have been processed into nanofibers with diameters ranging from 3 nanometers to several microns [6].

Electrospinning is an inexpensive process that can be easily scaled up, employing multiple spinnerets. It is surprisingly versatile in that almost any soluble polymer can be processed into nanofibers. Both conductive and dielectric polymer solutions have been successfully utilized. Melts can also be spun into fibers but usually result in larger fiber diameters [7]. Composite and hollow nanofibers, including nanofibers containing liquids have been produced by coaxial

electrospinning [8-10]. Continuous carbon and ceramic nanofibers have also been produced by modified processes [8,10-12]. Examples of several nanofibers that show promises for biomedical applications are shown in Fig. 2. A list of biocompatible polymers that have been electrospun shall be highlighted in the next section.

2.2. Fundamental Mechanisms of Jet Motion in Electrospinning

Electrospinning differs from conventional mechanical spinning used to produce synthetic fibers in the way the driving force is applied to the jet. In conventional spinning, mechanical force is applied at the end of the jet through a rotating mandrel. In electrospinning, volumetric electrical forces are applied to charged jet particles. Creation of liquid jets by an electrostatic field is a well-known phenomenon [13,14]. Such jets have been used in industrial processes, e.g. electrostatic atomization and ink-jet printing. However, electrospinning differs qualitatively from these electrically driven processes involving low-molecular weight liquids. In the latter processes, the initially continuous jets break-up into droplets at a short distance from the jet starting point [13,14]. The break-up is caused by varicose or Raleigh instability. This instability is persistent and is the reason most liquids can be “atomized” into micron-sized droplets through jet creation. It is also the reason, why relatively little effort has been devoted over the years to study jet diameter variation in these processes at a substantial distance from jet origination.

Electrospinning involves high molecular weight polymer liquids. Polymer chain entanglement results in complex, non-linear rheological behaviour that complicates the analysis. This complex rheology coupled with the strength of extended polymer chains (chemical versus intermolecular bonds) suppress varicose instability and prevent jet break-up into droplets. Assisted by unusual jet instability, long drawing distances result in fine jets that ultimately solidify into nanofibers.

Modelling is essential for better understanding of this complex coupled process. For modelling purpose, the process can be broken into several essential subprocesses, i.e. jet initiation, steady-state spinning, and jet instabilities.

Jet initiation in electrospinning has been treated as a break-up of highly charged liquid meniscus [15]. Such meniscus deforms in the electric field until beyond a certain threshold field a fine jet is ejected from the meniscus. Usual energy-based analysis methods are not applicable to this problem due to the variable volume and charge of the meniscus. A new approach based on the asymptotic electromechanical analysis at the meniscus apex has been developed [15]. The general method can be used on dielectric and conductive polymer solutions. The resulting stability diagrams can then be used to predict jet initiation [16].

Steady-state electrospinning is the continuous process of straight jet motion from the origin towards the external electric field. The non-linear rheology of polymer fluids and the volumetric nature of electric forces come into play. Several models of electrospun jets have been developed recently [12,16]. Simple asymptotic exponents have been derived for various jet flow regimes [17]. The above models provide insight into jet stretching in the initial stages of the electrospinning process. Their results can be used as a starting point for jet instability analysis.

One of the major breakthroughs that has substantially improved our understanding of the electrospinning process is the discovery and explanation of “bending” or “whipping” instability [18-20]. This instability transforms initially straight jet segments into “bent” jets that assume spiral, helical, or serpentine shapes. The instability was discovered by analyzing high-speed videos of the process. In the past, conventional photographs of the process appeared to show massive jet splaying that started at a certain point down the jet stream and resulted in multiple

smaller jets deposited on substrates. The evidence seems so compelling that even now many publications continue to show splayed jets in their schematics. In reality, as seen on high-speed video frames, the apparent splayed jets are nothing but traces of multiple bent jet segments rapidly moving radially from the point of first bending instability [18]. The mechanism of this instability is driven by the transverse components of the internal electrical forces in the perturbed jet segments. Models of bending or whipping instabilities provide better insight into the process and lead to better process control. Splaying instability, though more rare, has also been observed in experiments and models. It is currently believed that jets instabilities may occur hierarchically at the decreasing scales in the electrospinning process. The instabilities intensify jet thinning and are therefore essential for production of ultrafine nanofibers.

In summary, electrospinning is a highly coupled process involving high-speed nonlinear electrohydrodynamics, complex rheology, and transport of charge, mass, and heat within the jet [6,21]. The process is characterized by massive jet instabilities that are persistent, occurring at multiple scales, and responsible for jet thinning. Despite recent advances on process analysis and modelling, much remains to be done. More sophisticated coupled models will provide deeper insights into the mechanisms of jet thinning and instabilities and will further facilitate process optimization.

2.3. Control of Nanofiber Diameter and Morphology

A major readout of the electrospinning process is the diameter of the fiber. So far, this is controlled mostly empirically [22-24], relying on variation of polymer concentration and molecular weight of the polymer. These parameters have great effect on polymer solution viscosity that results in different jet thinning. For most polymer systems, variation of these two parameters may produce nanofibers with diameters in the range of 50-1000 nm. The same parameters also largely determine the spinnability of the polymer solutions. Solutions with low polymer concentrations result in micronsize droplets (or particles, after solidification), as a result of varicose jet instability, similar to low-molecular weight liquids. The threshold concentration depends on the polymer molecular weight, the higher of which requires a lower concentration. Intermediate concentration and molecular weight values often result in beaded nanofibers (Fig. 3). It is likely that beading is initiated as varicose instability [25]. The fine polymer threads between the beads are among the smallest polymer nanofibers produced by electrospinning. For example, a fiber as small as 3 nm in diameter was observed [25].

Other fluid properties affecting jet flow in electrospinning are surface tension and dielectric and electrical properties. Variation of these parameters, for instance, by addition of surfactants or salts, can affect nanofiber diameter and morphology. For example, addition of salt and surfactant can result in the suppression of beading in the system with otherwise similar characteristics. Many other factors such as quality of solvent, diffusion coefficient, flow rate, and parameters affecting solvent evaporation play an important role in electrospinning and result in variation of nanofiber diameter and morphology. Temperature and other environmental conditions are also critical.

Cross-sectional shape of electrospun nanofibers is usually circular. However, ribbon-like fibers have also been produced [26]. An example of fine collagen ribbons produced by electrospinning in our laboratories (YD) is shown in Fig. 4. Ribbon morphology is most likely due to the collapse of rapidly solidified outer shell of electrospun jets. Another possible mechanism is non-axisymmetric jet instability originating from a perturbation of jet cross-sectional shape.

Nanofiber surface texture and porosity may be of critical importance for biomedical applications. Nanoscale surface texture can provide additional topographical cues for cell attachment and proliferation. Nanofiber porosity can affect specific fiber surface area that is

important for sensing or drug delivery functions. It has been shown that nanofiber surface and volumetric porosity and morphology can be controlled to a certain extent by the solvent type [27-30]. For example, the use of volatile solvents has led to substantial nanofiber porosity as shown in Fig. 5. Porous nanofibers as a result of phase separation in polymer-solvent systems have also produced [27-29]. Electrospinning of co-polymers can lead to unusual surface texture and properties [31]. Another technique that can produce nanofibers with surface or volumetric texture is blend spinning, followed by removal of selected constituents [27,32].

2.4. Control of Nanofiber Orientation

Many biomedical applications would benefit from the ability to produce aligned nanofiber assemblies. ECMs of a variety of tissues consist of aligned protein fibrils and bundles. Truthful reproduction of such ECMs using electrospinning would require nanofiber alignment. Massive hierarchical jet instabilities in electrospinning naturally result in random, nonwoven nanofiber mats or sheets. Substantial effort has been devoted in the recent years to the development of methods to achieve fiber alignment.

Conventional collection of nanofibers on the surface of a rotating drum or mandrel can produce thick nanofibrous sheets [33], but typically results in only partial nanofiber alignment, even at very high rotation velocities (Fig. 6). Nanofiber deposition onto the edge of a rotating disc (essentially, a narrow mandrel) resulted in a band of nanofibers with relatively high alignment [10]. However, it is difficult to use this method to produce high quality nanofiber sheets or 3D assemblies desirable for tissue engineering. Several methods of alignment based on electrical forces acting on charged jet segments have been explored recently [6,21]. One of the best methods is to use split collecting electrodes (gap method – Fig. 7a) [21,34] to produce aligned nanofibrous arrays or sheets (Fig. 7b). Sequential use of the method can result in highly customized 3D nanofibrous constructs as illustrated in Fig. 7c.

2.5. Electrospun Biocompatible Materials

The versatility of the electrospinning process has allowed for many different polymers, synthetic, natural or a blend of both, and even polysaccharides to be electrospun. Depending on the type of processing parameters, particularly the types of solvent used, and the concentration of polymer solution, fibers of different diameters can be obtained. There is increasing interest in studying hybrid composite fibers composed of a blend of natural and synthetic polymers. This is mainly due to the need to include both the superior mechanical properties of synthetic polymers and the biocompatibility of natural polymers into one single scaffold. Table 1 summarizes the various types of polymers and polysaccharide that has been electrospun. These biocompatible materials may find useful applications as tissue scaffolds or drug delivery vehicles.

In summary, nanofibers from biocompatible synthetic and natural polymers possess critical advantages for surface modification of implants and design of tissue engineering scaffolds. In contrast to patterned silicone or PDMS substrates, electrospun continuous nanofibers present a unique route for the development of practical *in vivo* applications. The process is versatile and provides a reasonable degree of control over the resulting size and morphology of the nanofibers. At the same time, continuous nanofibers can possess good mechanical properties to provide structural integrity for their assembly. Finally, in contrast to classical discontinuous nanomaterials such as carbon nanotubes and various nanorods, continuous electrospun nanofibers enjoy a macroscopic dimension that leads to easy handling, placement, processing into devices, and reduction of potential toxicity in *in vivo* applications.

3. Drug-Encapsulated Electrospun Fibers

Drug encapsulation in electrospun fibers is still relatively unexplored. The electrospinning process can be easily adapted to accommodate encapsulation of different bioactive agents. With a large surface area-to-volume ratio to facilitate efficient mass transport, drug-encapsulated fibrous scaffolds may offer efficient delivery to the seeded cells. In this section, we will review recent studies on incorporating controlled release functions in the form of low molecular weight drugs, plasmid DNA, proteins and glycosaminoglycan salts into electrospun fibers.

3.1. Fabrication

Solid or liquid drugs can be directly incorporated into electrospun nanofibers by composite electrospinning. Coaxial electrospinning can be used to encapsulate a drug-delivering solid or liquid core into a structural shell. The shell can be designed to produce controlled release *via* controlled diffusion properties, porosity, or biodegradability.

3.2. Types of Drugs

3.2.1. Low Molecular Weight Drugs—A variety of low molecular weight drugs has been electrospun, including lipophilic drugs such as Ibuprofen [35], Cefazolin [36], Rifampin [37], Paclitaxel [37] and Itraconazole [38]; and hydrophilic drugs such as Mefoxin [24,39] and tetracycline hydrochloride [40]. To date, the majority of the studies have been carried out with polyesters, particularly poly(lactic acid)s (PLA) because of their biocompatibility and FDA-approved status. Poly(ε-caprolactone) is another popular polyester because of its ease of processing. In general, a burst release is often observed when low molecular weight drugs are encapsulated in electrospun fibers. As a result, different attempts have been made to control the drug release kinetics. Such attempts include: conjugation of the drug to the polymer [35], alteration of drug-polymer interaction [35,39,40], use of enzymatically degradable polymer matrix [37], and alteration of mass transport to and from the scaffolds using an additional matrix [38].

3.2.1.1. Lipophilic Drugs: Ibuprofen, an anti-inflammatory agent, was loaded at 5wt% into electrospun poly (L-lactic-co-glycolic acid) (PLGA, LA:GA 75:25, Mw 8×10^4) and PLGA/PEG-g-chitosan (70:30 ratio) meshes in the form of a drug-polymer mixture by Jiang, *et al.* [35] for atrial fibrillation application. The drug was also conjugated to PEG-g-chitosan and electrospun at a drug loading level of 4.4wt% with PLGA, forming a drug-polymer conjugate. Drug release analysis carried out in 0.1M PBS at 37°C revealed a burst release of close to 50% from plain PLGA drug-encapsulated fibers, followed by a quick release of drugs by simple diffusion resulting in more than 85% drug release after 4 days of incubation. The rapid release was mainly associated with the lack of interaction between the drug and PLGA matrix [35]. By blending the drug with PEG-g-chitosan, the burst release was reduced to 20% and a sustained release was obtained for at least 16 days due to the ionic interaction between the carboxyl groups of the drug and chitosan. By conjugating the drug directly onto PEG-g-chitosan, a pseudo-linear drug release profile, with less than 40% drug release after 16 days of incubation was obtained. This is an excellent example of how physical and chemical interactions between the drug and the polymer matrix can be manipulated to overcome the rapid release kinetics of electrospun fibers.

Cefazolin, a broad-spectrum antibiotic was electrospun with PLGA 50:50 at different loading levels of 0%, 10% and 30% [36]. By observing the resulting fiber morphology, the authors optimized the electrospinning parameters accordingly for drug encapsulation. The authors observed that drug-loaded fibers possessed larger diameters than plain fibers, with drug-loaded

fibers having an average diameter ranging between 450 and 500 nm. The drug release kinetics of Cefazolin, however, was not evaluated.

Rifampin, a drug for tuberculosis treatment was encapsulated in PLLA electrospun fibers at loading levels up to 50wt% [37]. Incubation of the fibers with 15 and 25wt% of rifampin in 0.05M Tris-HCl, with and without proteinase K, at 37°C revealed that in the absence of proteinase K, no drug release was observed. Degradation of PLLA fibers by proteinase K resulted in a constant drug release rate, indicating that drug release from PLLA fibers occurred *via* polymer degradation instead of diffusion. This can be easily explained by the poor water solubility of Rifampin. Electrospinning of the anti-cancer drug, Paclitaxel, was also carried out. The drug release profile of Paclitaxel, however, was not reported [37].

Itraconazole, a broad-spectrum antifungal agent loaded in hydroxypropylmethylcellulose (HPMC) at 20 and 40% w/w was electrospun [38]. The *in vitro* drug release kinetics was studied in 0.1N HCl at 37°C, under a rotation of 100rpm using various forms of electrospun fibers, namely, free fibrous mesh, manually folded mesh, mesh inserted into a hard gelatin capsule size 0 and mesh enclosed in a metal spiral. The results indicated that drug release was negligibly altered by the change in drug loading level and electrical potential applied during electrospinning. An initial burst release, followed by a complete drug release within 500 minutes of incubation in HCl was observed. By obstructing the mass transport to and from the fibrous mesh through the encapsulation of the mesh in either a gelatin capsule, or a metal spiral, drug release was sustained for up to 1500 minutes. However, such an approach does not take advantage of the structural features of a fibrous mesh.

3.2.1.2. Hydrophilic Drugs: Mefoxin (Cefoxitin sodium), a general antibiotic was loaded at 1wt% in poly(D-lactic acid) (PDLA) [24] and 1 and 5wt% in PLGA or a mixture of PLGA/PEG-b-PLA diblock copolymer [39] by electrospinning. Release studies for the PDLA and PLGA fibers were conducted in PBS at room temperature and in water at 37°C respectively. Similar to the observations made by Jiang, *et al.* [35], both studies revealed an initial burst release of drugs from the polyesters within the first 3 hours of incubation (more than 80% drug release from PDLA; 40% drug release for 1wt% loading and 70% drug release for 5wt% loading from plain PLGA fibers; and 50% drug release at 5wt% loading from PLGA-PEG co-polymers). Drug encapsulated at a theoretical loading efficiency of over 90% in PDLA was completely released within the first 48hr. The burst and rapid release of the drug was related to the salt form of the drug and the lack of interaction between the drug and the polyesters, such that most of the drug was located either on or near the surface of the fibers [24]. In the presence of PEG, Mefoxin may be encapsulated within the hydrophilic block of PEG-b-PLA, hence reflecting a more sustained release of the drug (about 27% of drug continuously released over a week after initial burst). A test for the bioactivity of the drug was also carried out using *S. aureus* bacteria. The encapsulated drug maintained its bioactivity after the electrospinning process as demonstrated by its ability to inhibit the growth of the bacteria for up to 24 hours [39].

Tetracycline hydrochloride was encapsulated at 5wt% in poly(ethylene-co-vinyl acetate) (PEVA), PLA and a 50/50 blend of the two polymers *via* electrospinning, with the aim of applying the fibers to the treatment of periodontal disease [40]. Drug release kinetics observed from placing the drug-loaded fibrous meshes into tris buffer showed that, similar to the observations made by Zong, *et al.* [24], an initial burst release was observed from the PLA fibers. Thereafter, drug release was negligible over the next 50 hours, which was similar to the observations made by Zeng, *et al.* [37], whereby drug release was not observed from PLA fibers in the absence of proteinase K. The release kinetics was probably due to the release of drugs on the surface of the PLA fibers, and the subsequent restricted diffusion of the drugs from the partially crystalline PLA fibers. The drug release was further hindered by the slow

hydrolytic degradation rate of PLA, which probably was negligible within the period of the study. Electrospun PEVA and polymer blend, however, showed a more continuous release of drug, with 65% and 50% of the drugs released within 120 hours, respectively. The drug release profiles were also compared to that of Actisite® periodontal PEVA fiber that was loaded with 25wt% of tetracycline hydrochloride. After the initial burst release, the drug release rate of electrospun PEVA and polymer blend was similar to that of Actisite. Drug release from these fibers was *via* molecular diffusion of the dissolved drug, since no obvious porosity was seen on the fibers after drug release. A comparison of the drug release rate was also made with solvent cast film of PEVA, PLA and the polymer blend, revealing a much faster release rate from the electrospun fibers due to the increased surface area provided by the fibers.

3.2.1.3. Antimicrobial Agents: Melaiye, *et al.* [41] utilized Tecophilic, a family of hydrophilic polyether-based thermoplastic aliphatic polyurethanes, to encapsulate silver (I) –imidazole cyclophane gemdiol complex at loading levels of 25wt% and 75wt% *via* electrospinning. Although the actual release kinetics of the silver complex was not evaluated, the antimicrobial activity of the fibrous mesh was found to sustain for over a week. Evaluation of the bactericidal activity of the encapsulated silver by incubation with various species of prokaryotes (*Escherichia coli*, *Pseudomonas aeruginosa* and *Staphylococcus aureus*) with the fibrous mesh overnight at 35°C revealed that the fibrous mesh enhanced the antimicrobial activity of the silver(I)-heterocyclic carbene complex on micro-organisms. It was also found that a much lower concentration of silver complex was required than silvadene, a widely used clinical drug, to kill bacteria at a much faster rate [41].

3.2.2. Plasmid DNA—Only one study has been reported on the use of electrospun fibers for gene delivery [42]. The authors encapsulated pCMVβ plasmid DNA by electrospinning in the polymer blend of PLGA 75:25 and PLA-PEG block copolymer at various weight ratios. The study of the DNA release kinetics was subsequently carried out in Tris-EDTA buffer at 37°C over a period of 20 days. Close to 68-80% of the encapsulated DNA was released within the first 5 days of incubation, with the release profile plateauing thereafter for the remaining 15 days. Analysis of the release kinetics at early time points revealed a burst release within the first 15min of incubating the scaffolds, and a dramatic decrease in DNA release after the initial 2 hours of incubation. The burst release of the DNA was most likely related to the portion of DNA located on the surface of the fibers [42]. The rate and extent of DNA release decreased with an increasing amount of block copolymer PLA-PEG. Therefore, this study, along with the observations made by other researchers [24,35,39,40], emphasizes the importance of drug-polymer interactions or drug partitioning in controlling drug release rates. With the evaluation of the structural integrity and bioactivity of the released DNA by gel electrophoresis and transfection of MC3T3 cell, the authors also demonstrated that the released DNA maintained at least partial bioactivity after electrospinning.

3.2.3. Proteins—The encapsulation of proteins *via* electrospinning may appear to be a challenging task due to the fact that denaturation of these macromolecules often occurs easily, especially upon being subjected to harsh processing conditions such as high electrical potential and the exposure to organic solvents. Nonetheless, two studies have successfully demonstrated the possibility of encapsulating and releasing bioactive proteins from electrospun fibrous meshes.

Similar to most other drug encapsulation studies, whereby a homogeneous drug-polymer solution is electrospun, Zeng, *et al.* [43] encapsulated bovine serum albumin (BSA) (0.01wt %) and Luciferase in poly(vinyl alcohol) (PVA) by electrospinning a homogeneous mixture of protein-polymer aqueous solution. Protein release kinetics was assessed by incubating electrospun fibers in water at either 4, 20 or 37°C. PVA/BSA fibers were incubated at 20°C due to the fact that PVA quickly solubilizes in water at 37°C, thereby giving a rapid drug

release. In order to overcome the problem of PVA dissolution in water, the fibers were coated with poly(p-xylylene) so as to limit the release of proteins from the fibrous scaffolds. Incubation of the coated mesh in water at 37°C yielded a sustained release of the drug for more than 20 days, with the protein release rate solely controlled by the water permeability of the polymer coating. Contradictory to the fact that protein was continuously released from coated fibers for more than 20 days at 37°C, the test for the bioactivity of the electrospun protein using recombinant Luciferase enzyme was carried out at 4°C for only 1 day. Although the analysis indicated that the encapsulated enzyme retained its bioactivity, it did not indicate if the fibers succeeded as a form of protection to prolong the half-life of the protein at room temperature or physiological conditions and also to release the encapsulated enzyme in a sustained manner.

In another study, Chew, *et al.*, [44] electrospun a heterogeneous protein-polymer solution for protein encapsulation. The electrospinning solution comprised of an aqueous solution of human β-nerve growth factor (NGF), which was stabilized with bovine serum albumin (BSA) as a carrier protein, and an organic solution of a copolymer of ε-caprolactone and ethyl ethylene phosphate (PCLEEP) in dichloromethane. Partially aligned protein encapsulated fibers were obtained, with the theoretical loading levels of NGF and BSA being 0.0123 and 4.08% respectively. Incubation of the protein encapsulated fibers in serum-free RPMI medium yielded a sustained release of NGF *via* diffusion for at least 3 months. The bioactivity of the electrospun NGF was also assessed through PC12 neurite outgrowth assay, which indicated that the bioactivity of the electrospun NGF was retained, at least partially, throughout the period of sustained release. The study demonstrated the feasibility of encapsulating proteins *via* electrospinning to produce biofunctional tissue scaffolds.

3.2.4. Glycosaminoglycan—Tri-*n*-butylamine salt of heparin (heparin-TBA) was loaded at 1, 5 and 10wt % into a copolymer, poly($_L$-lactide-*co*-ε-caprolactone) (PLCL 50:50), in attempt to immobilize and sustain release heparin from the polymeric fibrous scaffold for vascular graft engineering applications [45]. The tri-*n*-butylamine salt was used instead of heparin so that the amphiphilic salt of the glycosaminoglycan may be soluble in the polymer solution of PLCL and 1,1,1,3,3,3-hexafluoroisopropanol. Heparin-TBA phase separated within the PLCL nanofibers, resulting in small domains of heparin-TBA being well-dispersed throughout the PLCL matrix, and about 2-5% of the total salt content being localized on the surface of the fibers. *In vitro* release kinetics carried out in PBS at 37°C revealed an initial ~20-30% burst release within the first 12 hours, followed by a sustained release for 4 weeks. The release mechanism was attributed to the degradation of the copolymer due to the fact that many fibers appeared disconnected and thin after 4 weeks of incubation, although the surface of the fibers remained smooth. The bioactivity of the immobilized and released heparin-TBA was, however, not evaluated, although the bioactivity of the salt was, prior to electrospinning.

3.2.5. In vivo application—The possibility of encapsulating a wide variety of drugs in different polymers by the simple process of electrospinning suggests that electrospun drug-encapsulated meshes may be able to find broad applicability as controlled release scaffolds, particularly in tissue engineering applications. Zong, *et al.* [46] studied the use of mefoxin-loaded electrospun fibrous meshes as scaffolds for the prevention of postsurgery induced abdominal wound adhesion in a rat model. The drug was incorporated into electrospun PLGA 75:25 or a PEG-PLA diblock copolymer. Plain and drug-encapsulated meshes were then placed between the defects on the abdominal wall and cecum of the rats for 28 days. The prevention of adhesion was significantly improved with the inclusion of the electrospun fibers, presumably due to the presence of a physical barrier provided by the fibers. It was, however, unclear whether there was a significant difference in the prevention of adhesion between the plain and mefoxin-loaded mesh. Nonetheless, this is the first example of an *in vivo* biomedical application of electrospun fibrous mesh.

In general, it has been demonstrated that regardless of the nature of the drug, whether low molecular weight, protein, or plasmid DNA, the bioactivity of the drug can be retained at least partially after electrospinning. Other than a bottom-up approach of using macromolecular self-assembly, it is difficult to introduce biofunctionality into nanostructures. Electrospinning, with its capability of fabricating nanofibers, represents an excellent technique of forming biofunctional nanostructures. Coupling the biofunctionality with the simplicity and broad applicability to a wide range of polymers, electrospinning can be expected to find many interesting biomedical applications in the near future.

4. Electrospinning for Tissue Engineering Applications

Being an emerging field applied to tissue engineering, electrospinning has yet to make a significant impact on *in vivo* applications. Although many different polymeric scaffolds and cell types have been studied, the bulk of the research thus far is still restricted to preliminary, qualitative analyses of the cytocompatibility of the electrospun materials in terms of cell adhesion, proliferation and changes in cell morphology. However, increasing attention is being paid to the more quantitative evaluation of the changes in cellular functions as a result of the topographical cues provided by the nanofibrous scaffolds.

4.1. Cardiovascular Tissue Engineering

4.1.1. Smooth Muscle Cells—Xu, *et al.* [47] demonstrated the potential of poly(L-lactide-co-ε-caprolactone) [P(LLA-CL)] (75:25) electrospun fibrous scaffolds (fiber diameter, φ, = 400-800nm) as a material for the engineering of vascular grafts. After 7 days of culture, the human coronary artery smooth muscle cells (SMC) integrated well into the scaffold, reaching close to 90% confluence. The SMCs also maintained their phenotypes as evidenced by being stained positively for α-actin and myosin.

Similarly, using human coronary artery smooth muscle cells, Venugopal, et.al. [48] compared the biocompatibility of electrospun scaffolds made of collagen type I (φ 300 – 375nm) and poly(caprolactone) (φ 661 – 700nm) in terms of cell proliferation, cell adhesion and cell growth rate assays after 3 days of *in vitro* cell culture. They concluded that while all scaffolds promoted cell-matrix and cell-cell interactions and preserved the phenotypic morphologies of SMCs, PCL scaffolds with collagen type I coating was the preferred choice. In such combination, the PCL provides the desired mechanical characteristics and collagen the cytocompatibility.

With a novel approach, Stankus, et.al. [49] evaluated the feasibility of integrating high density of vascular smooth muscle cells directly into poly(ester urethane)urea (PEUU) fibrous scaffolds (φ not stated) during the electrospinning process, in order to obtain a well integrated, three-dimensional distribution of cells throughout the fibrous scaffold. Two orthogonally-positioned separate supplies of polymer and cells were used during the electrospinning process, and despite exposure to a large electric field, cells electrosprayed from cell culture media were found to be more than 90% viable after the fabrication process. Cellular constructs of thickness between 300 to 500μm were obtained and cells proliferated under 7 days of transmural perfusion culture, as compared to static culture, where cell number remained unchanged. Cellular morphological analyses also revealed healthier-looking cells uniformly located throughout the scaffold under perfusion culture as opposed to static culture. Comparing cells integrated into 100μm thick constructs to cells seeded on TCPS for 7 days under static culture conditions, integrated cells appeared to have a larger increase in cell number. Although some extent of cellular orientation may be achieved *via* PEUU fiber alignment during the fabrication process, the integration of cells, however, decreased the mechanical strength of PEUU scaffolds.

With the use of electrospun PLA fibrous meshes (φ ~10μm) and collagen type I fibers (φ=100-250μm), Stitzel, *et. al.* [50] fabricated a prototypic vascular graft. The authors demonstrated that the vascular graft prototype was able to support the growth of human aortic SMCs, with confluent layers of SMCs being observed in the luminal and external surfaces of the vascular graft after 10 days of culture. The SMCs were also observed to align and organize in the presence of collagen I fibers, as opposed to cells that were seeded on grafts without collagen I fibers. The authors attributed the cell alignment to the stress exerted by the collagen fibers, which may mimic the stress of a closed section of an artery, thereby aligning the cells. The work was further expanded with the fabrication of a prototypic vascular graft composed of a mixture of collagen type I, elastin and poly($_{D,L}$-lactide-*co*-glycolide) (PLGA) electrospun nanofibrous scaffold (φ 0.720 ± 0.35μm) [51], in attempt to more closely mimic the mechanical properties and material composition of a blood vessel. Bovine SMCs were used to assess the *in vitro* biocompatibility of the material by seeding the cells in wells along with the electrospun scaffolds and assessing cell viability and proliferation up to 7 days, instead of directly seeding the cells on the electrospun scaffolds. Nonetheless, cell attachment was also evaluated by co-culturing bovine endothelial cells and SMCs on the inner and outer surfaces of the electrospun prototypic vascular graft respectively. Confluent layers of cells were observed after 3-4 days of culture, demonstrating the biocompatibility of the material. *In vivo* biocompatibility of the scaffold was also carried out through subcutaneous implantation of the fibrous mesh. The evaluation of other important properties of a vascular graft, such as the leakage of fluids from the graft and graft patency still remain to be carried out.

Since these studies with SMCs have focused only on cell-substrate interactions, one may only conclude that electrospun fibrous scaffolds may serve as a promising scaffold for the culture of SMC. The exact benefit of using these scaffolds, particularly nanofibrous scaffolds, for vascular tissue engineering applications as opposed to scaffolds of other structures remain to be addressed.

4.1.2. Endothelial Cells—The potential of electrospun poly(L-lactic acid) (PLLA) fibrous scaffolds in supporting the growth of human vascular endothelial cells (ECs) was evaluated by Xu *et al.* [52]. Electrospun scaffolds comprising of fibers with diameters of 235 ± 71 nm and 3500 ± 854 nm respectively were studied in parallel with tissue culture polystyrene (TCPS) and PLLA solvent-cast film as controls. Immunostaining for cell adhesion protein, CD31, revealed that ECs appeared to adhere less well onto the electrospun scaffolds, maintaining a rounded morphology, as compared to the typical cobblestone appearance of ECs when seeded onto flat surfaces. Cell proliferation also appeared to be better on flat surfaces, as compared to the fibrous scaffolds. However, no significant differences in cell behavior were observed in cells cultured on the micro- and nano-fibrous scaffolds.

In a separate study, the same group demonstrated good interaction and integration of human coronary artery ECs with poly($_{L}$-lactide-co-ε-caprolactone) [P(LLA-CL)] (75:25) scaffolds (φ = 400 – 800nm) [47]. The ECs reached close to 75% confluence after 7 days of culture. Immunostaining for CD31 and CD62E in ECs demonstrated that the cells maintained their phenotypes. The study demonstrated the potential of P(LLA-CL) fibrous scaffolds as a material for vascular grafts. However, since the study was done in the absence of a flat surface control, it was inconclusive as to whether the structure of the nanofibers, hence surface roughness, affected cell attachment and proliferation as compared to a smooth surface.

Kwon *et.al.* [53] studied the effects of fiber diameters on the adhesion, proliferation and morphology of human umbilical vein endothelial cells (HUVECs). Electrospun micro- and nano-fibrous scaffolds of a copolymer of L-lactide and ε-caprolactone, PLA-CL 50/50, were obtained by varying the processing parameters. The authors observed that cell adhesion and proliferation were better on the small-diameter fiber meshes (0.3 and 1.2μm diameter fibers).

The cells also spread and elongated along the small-diameter meshes. In contrast, cells seeded on the 7μm diameter fibrous mesh showed reduced cell adhesion, restricted cell spreading and no signs of proliferation. Together with the observations made by Xu *et al.*[52], it appears that a threshold fiber diameter may exist between 3.5 to 7μm to significantly affect the adhesion and morphology of the cultured ECs.

Still using a similar polymer, He, *et.al.* [54] fabricated nanofibrous scaffolds (φ = 470 ± 130nm) from a random copolymer of poly($_L$-lactic acid)-*co*-poly(ε-caprolactone), P(LLA-CL 70:30). In order to enhance biocompatibility of the scaffold, collagen type I was used as the surface coating, after air plasma treatment of the scaffolds. Preliminary studies to evaluate the feasibility of the fibrous mesh as a tissue scaffold were carried out by analyzing the morphology, viability and adhesion of human coronary artery endothelial cells on the fibrous mesh. Cells cultured on plain P(LLA-CL) mesh adopted a rounded morphology, had a lower viability after 3 days of culture and adhered less well to the scaffold as compared to the collagen-coated mesh. ECs seeded on the collagen-coated mesh, however, had similar morphology and extent of cellular attachment as compared to TCPS, indicating the importance of protein adsorption onto the scaffold. Immunostaining for CD31 demonstrated the preservation of EC phenotype on collagen-coated scaffolds and TCPS, but similar analysis was not carried out on the plain P(LLA-CL) scaffolds. The similarity in cellular morphology, attachment, preservation of phenotype, and the lower level of cell viability when cultured on collagen-coated meshes as compared to TCPS, however, appeared to argue against the need of the use of nanofibrous scaffolds for EC culture. Also, similar to the work by Xu, *et.al* [47], the absence of a flat P(LLA-CL) surface as a control renders conclusions difficult regarding the uniqueness or advantage of a nanofibrous scaffold as compared to a flat surface.

A similar approach was taken by Kwon and Matsuda [45] to combine the copolymer poly($_L$-lactide-*co*-ε-caprolactone) (PLCL 50:50) with collagen type I. However, instead of serving as a coating, collagen was blended into PLCL and electrospun into a composite fibrous mesh (φ = 120-520nm). The advantage is perhaps the ease of introducing collagen in the single-step process of electrospinning, as opposed to the multiple step approach taken by He, *et.al* [54]. HUVECs were used to evaluate the potential of the composite mesh as a tissue scaffold by observing the cell adhesion and proliferation for up to 5 days of culture on the mesh. PLCL scaffolds coated with fibronectin and blended with small amounts of collagen (5 and 10wt%) were found to increase cell attachment, spreading and proliferation as compared to plain PLCL meshes. Scaffold shrinkage due to large amounts of collagen present (30 and 50wt%) appeared to offset the advantages of blending collagen by resulting in a much lower number of cells on the scaffolds after 5 days of culture.

Along the same line of developing electrospun fibrous scaffolds into vascular grafts, human coronary artery endothelial cells were cultured on electrospun poly(ethylene terephthalate) (PET or Dacron) nanofibrous scaffolds (φ = 200-600nm) [55]. Since PET is frequently used as replacements for large-diameter arteries, the authors wanted to evaluate the feasibility of using PET electrospun fibrous scaffolds for EC culture as small diameter vascular grafts. ECs cultured on TCPS, PET nanofibers and PET nanofibers with grafted gelatin were compared in terms of cell attachment, proliferation and morphology. The authors found that gelatin grafting onto PET fibers was necessary to achieve cell attachment. However, cell proliferation and viability on PET, whether coated or uncoated were lower than that on TCPS. Immunostaining showed that the expression of various adhesion molecules, namely CD31, CD106 and CD54 remained in the cells when cultured on the electrospun scaffolds, suggesting the preservation of the EC phenotypes. The analysis, however, also indicated a decrease in expression of CD31 in cells cultured on electrospun scaffolds as compared to cells on TCPS. Although the authors demonstrated that PET fibrous scaffolds can support EC growth to a certain extent, the scaffolds appear to be not as ideal for EC phenotype expression as compared to TCPS. Similar to the

results obtained by Xu *et al.*[52], ECs appeared to prefer smooth surfaces such as TCPS rather than the rough surfaces provided by the PET nanofibrous scaffolds. Since a comparative study on smooth PET films has yet to be performed, the influence of surface chemistry on cell adhesion and proliferation cannot be eliminated.

In order to evaluate the biocompatibility of their vascular graft phenotype, which comprised of a mixture of collagen type I, elastin and poly($_{D,L}$-lactide-*co*-glycolide) nanofibers ($\varphi = 0.720 \pm 0.35$ μm), the viability and proliferation of bovine endothelial cells were evaluated by Stitzel, *et.al.* [51], by seeding the ECs in wells along with the electrospun scaffolds. Cell attachment was also evaluated by co-culturing bovine smooth muscle cells with the ECs in the external and luminal surfaces of the vascular prototype respectively. Results indicated that the material was biocompatible and supported cell attachment for up to 7 and 4 days respectively.

With the studies on EC interaction with electrospun fibers put together, it appears that ECs adhere and proliferate better on smooth surfaces. When cultured on textured surfaces provided by electrospun fibers, there appears to be a threshold diameter, below which the effects on cell adhesion, proliferation and morphology may be negligible. This threshold diameter may lie between 3.5 to 7μm.

4.1.3. Primary Cardiomyocytes—Primary cardiomyocytes were cultured on three different electrospun aligned fibrous scaffolds made of PLA, blend of PLA and PLGA 10:90 (25/75 wt%), or blend of PLGA 75:25 and PEG-PLA (85/15wt%) [56]. The authors observed that the increase in hydrophilicity of the substrate with the inclusion of PEG resulted in structurally compromised cell clumps. Attempts to increase the scaffold degradation rate, with the inclusion of PLGA 10:90 also led to cells clustering together, losing their spatial organization. Cell density, therefore, was the highest on PLLA fibers, followed by PLGA 10:90 and lastly PEG-PLA. Functional studies of the cells were also carried out using optical mapping of electrical activity of the cells. Cells on PLLA performed better than those on the other two scaffolds [56], by being able to follow external pacing rates up to 6 Hz (as opposed to 2Hz or less on the other scaffolds) with shorter action potential durations. The study suggested the possibility of using aligned electrospun fibrous scaffolds for cardiac patch engineering.

4.2. Neural Tissue Engineering

4.2.1. Neuronal Stem Cells—Electrospun poly(L-lactic acid) (PLLA) micro and nanofibrous scaffolds comprising of either aligned or random fibers have been investigated as a scaffold for the culture of neonatal mouse cerebellum C17.2 stem cells (NSC) [57]. The study evaluated the effects of fiber alignment and fiber diameter on the morphology and proliferation of the neuronal stem cells. The samples used in the study included random nanofibrous mesh (average $\varphi = 700$nm), aligned nanofibrous mesh (average $\varphi = 300$nm), random microfibrous mesh (average $\varphi = 3.5$μm) and aligned microfibrous mesh (average $\varphi = 1.5$μm). The neuronal stem cells attached well onto all fibrous scaffolds, with extensive neurite-like outgrowth. They elongated and aligned in the direction of the aligned fibers, but adopted a random morphology on random fibrous scaffolds, thus demonstrating the contact guidance provided by the structure of the aligned fibers. Cells were also observed qualitatively to elongate more on nanofibers as compared to microfibers, regardless of fiber orientation. While this study suggests the intriguing effect of nanoscale features on NSC neurite outgrowth, electrospinning will always produce fibers with a size dispersity in diameter and imperfect alignment. It would therefore be challenging to compare the difference between cellular behavior on electrospun microfibers and nanofibers in a quantitative manner. Definitive conclusion would have to await studies performed on regular nanoscale features fabricated by other nanofabrication techniques, such as nanolithography and nanoimprinting. If the effect of nanotopography on NSC differentiation

can be substantiated, it would have profound implications on the design of neural tissue engineering scaffolds.

4.3. Musculoskeletal Tissue Engineering

4.3.1. Myogenic Cells and Human Satellite Cells—DegraPol, a degradable block polyesterurethane was electrospun into microfibrous scaffolds (average φ = 10μm) for the potential application of muscle regeneration [58]. Myogenic cells and human satellite cell adhesion and proliferation were separately observed after 7 days of culture, with myogenic cells staining positively for skeletal myosin heavy chain expression but negatively in the satellite cells. The multi-nucleation of the myogenic and satellite cells on the scaffold indicated the possibility of using these scaffolds for skeletal muscle tissue regeneration. However, cell proliferation on the scaffolds appeared to be inferior to that on TCPS. While the ability of these scaffolds to support cell differentiation to skeletal muscle tissues remains unclear, these scaffolds are reportedly cell compatible.

4.3.2. Osteoblasts—Polycaprolactone/$CaCO_3$ composite electrospun nanofibrous scaffolds (φ = 900 ± 450nm and φ = 760 ± 190nm) have been used to culture human osteoblasts [59]. The composite scaffolds were cyto-compatible. Cell morphology analysis revealed an increase in granulates formation in cells seeded on composite fibers comprising of a higher percentage of $CaCO_3$, suggesting that differentiation of the osteoblasts might have occurred to yield mineralization. Cell proliferation, however, appeared to be lower on the composite fibers with higher $CaCO_3$ content, probably due to the fact that the cells were undergoing differentiation [59].

Human osteoblast-like cell line (MG-63) was used to evaluate the feasibility of utilizing chitosan-poly(ethylene oxide) composite fibers as a tissue engineering scaffold [60]. The only analysis carried out was the observation of cell-matrix interaction under scanning electron microscope, which revealed that osteoblasts adhered to surfaces by discrete filopodia and that the microvilli of cells appeared to attach and grow along the electrospun fibers.

In order to understand the behavior of MC3T3-E1 mouse calvaria-derived osteoprogenitor cell line on different substratum topographies, TCPS, spin-coated PDLLA and PEG-PDLLA were used in parallel with PDLLA, PLLA, PEG-PDLLA and PEG-PLLA electrospun fibers [61]. The authors found that alkaline phosphatase activity was not affected by the topography of the scaffold, but cellular morphology was influenced. Cells seeded on electrospun fibers generally had a smaller projected area than cells on flat surfaces, except for cells cultured on electrospun scaffolds with fibers of an average diameter of 2.1μm, in which case they were possessed high aspect ratio, similar to the case of contact guidance. The authors also found that the effect of osteogenic factors was prominent. Cell proliferation was lower on fibrous scaffolds as compared to smooth surfaces when osteogenic factors were left out of the cell media, but the opposite was seen in the presence of osteogenic factors. Cell density was also found to increase with increasing fiber diameter. The study demonstrated that cell proliferation and morphology may be affected by the surface topography of a substrate but it has not clearly established the pros and cons of using electrospun fibrous mesh as a tissue scaffold

3.3. Chondrocytes

Adult human articular chondrocytes [62] have been cultured on chicken sternae collagen type II nanofibrous scaffolds (average φ= 496nm (min 70nm max 2.74μm)). The chondrocytes adhered, proliferated and infiltrated the scaffold, indicating good cell biocompatibility of the electrospun collagen type II scaffolds.

With a similar objective to evaluate the biocompatibility of chitosan-PEO blended fibers, a human chondrocyte-like cell line (HTB-94) was cultured on the fibrous meshes (φ~ few microns to ~40nm) [60]. Analyses of cell attachment, morphology and viability revealed good cell adhesion and interaction with the fibrous mesh and seemingly larger amount of live cells on the mesh as compared to a solvent-cast film of similar material composition. The study indicated the biocompatibility of the scaffold and the advantage of nanofibrous scaffolds over flat surfaces.

Using a random non-woven mesh of PCL nanofibers (average φ = 700nm), the functionality of the 3-dimensional structure of electrospun nanofibrous scaffolds in controlling chondrogenic differentiation in fetal bovine chondrocytes (FBCs) [63] was evaluated. The de-differentiated chondrocytes were able to re-differentiate without the addition of growth factors after 21 days of cell culture, suggesting that the electrospun fibers may be able to stimulate the seeded cells to release the endogenous growth factors necessary for chondrocytic differentiation. Cells seeded on the fibers proliferated in the presence of serum. However, differentiation of the cells was encouraged in serum-free medium. This suggested that the PCL nanofibrous scaffolds can support both cellular proliferation and differentiation. Control over cell proliferation and differentiation may be achieved merely by the switching of cell culture medium from serum to serum-free medium. Cartilage-associated genes in FBCs, such as collagen type II, collagen IX, aggrecan, and COMP were all upregulated on PCL fibrous scaffolds as compared to cells seeded on TCPS. Changes in cellular functions was also assessed by Alcian Blue staining, revealing a higher amount of sulfated matrix production in the FBCs [63] seeded on electrospun scaffolds.

While most of the studies on the use of electrospun fibrous scaffolds for orthopedic implant applications revolves around the evaluation of the cyto-compatibility of the scaffolds, the study by Li, *et al.* [63] illustrated the potential of electrospun fibrous scaffolds for chondrogenic differentiation. Electrospun scaffolds, as shown by Li, *et al.* [63] may have distinct advantages over other 3-D scaffolds that are currently used for chondrogenic differentiation. Firstly, unlike other scaffolds such as hydrogels, chondrocytes cultured on electrospun scaffolds may not require the addition of growth factors for cartilage tissue development, and secondly, nanofibrous scaffolds have superior mechanical integrity as opposed to hydrogels [63].

4.4. Stem Cell Engineering

4.4.1. Human Bone Marrow-Derived Mesenchymal Stem Cells (MSCs)—The cell biocompatibility of electrospun fibrous scaffolds with MSCs were demonstrated using PLGA 85:15 electrospun nanofibrous scaffolds (φ = 500 to 800 nm) [64] and Bombyx mori silkworm silk fibroin/PEO composite electrospun scaffolds (average φ = 700±50nm) [65] in two separate studies by evaluating the attachment and proliferation of MSCs in the scaffolds.

In a separate, more in-depth study, PCL nanofibrous scaffolds (φ average = 700nm) were utilized as a 3-D scaffold for chondrogenic differentiation of MSCs. The effectiveness of electrospun scaffolds in enhancing chondrogenic differentiation was evaluated by comparing with high density cell pellet culture in the presence of TGF-β1 [66]. Cell proliferation and the level of MSC chondrogenesis in nanofibrous scaffolds were found to be comparable, and in some cases, better than that in cell pellet culture. Cells were also observed to adopt a cartilage-like morphology in the fibrous scaffolds. While collagen type II expression level was similar in both cell pellet culture and fibrous scaffolds, collagen type IX expression was upregulated on nanofibrous scaffolds. A continuous synthesis of sulfated glycosaminoglycans was also observed throughout the entire duration of cell culture. These results demonstrated the effectiveness of electrospun fibrous scaffolds in supporting chondrogenesis of MSCs, probably due to the microstructural resemblance of the fibrous scaffolds to native collagen fibrillar matrix [66].

In a separate study using the same PCL nanofibrous scaffolds, the same group continued to evaluate the potential of electrospun fibrous meshes in supporting and maintaining the multilineage differentiation of MSCs. In showing that MSCs were able to differentiate along adipogenic, chondrogenic and osteogenic lineages in specific differentiation media [67], the authors concluded that indeed the conducive 3-D structure of electrospun nanofibrous scaffold was versatile enough to support such multilineage differentiation.

4.4.2. Bone Marrow Stromal Cells (BMSCs)—Cell biocompatibility of gelatin/PCL composite fibrous meshes (φ~ 1 μm) were evaluated by seeding rabbit bone marrow stromal cells (BMSCs) onto the scaffold for 7 days [68]. BMSCs were observed to stretch and spread on the composite scaffolds instead of retaining a rounded morphology, as seen on plain PCL scaffolds. Cells were also observed to penetrate a greater depth (114μm) into the composite scaffold, as opposed to only 48μm from the surface of plain PCL scaffolds. The study demonstrated the enhanced mechanical properties of the hybrid scaffold over natural polymeric scaffolds and its improved biocompatibility over synthetic polymeric scaffolds.

The studies highlighted above underline the potential of electrospun nanofibrous scaffolds for stem cell engineering. Electrospun fibrous scaffolds, besides providing structural support to the cultured stem cells, may also provide the topographical signals to influence cell differentiation, particularly through the nanostructural architecture provided by the fibers.

4.5. General Evaluation of Cytocompatibility of Electrospun Fibrous Scaffolds

Various other cell types have also been cultured on electrospun fibrous scaffolds with the aim to evaluate the cell biocompatibility of the scaffolds. Li, *et al.* [64] cultured BALB/c C7 mouse fibroblast cells on PLGA 85:15 nanofibrous scaffolds (φ = 500 to 800 nm). Min, *et al.* [69, 70] cultured primary normal human gingival fibroblasts, oral keratinocytes, and epidermal keratinocytes on nanofibrous silk fibroin scaffolds (average φ = 80nm). Lastly, Khil, *et al.* [71] cultured MCF – 7 mammary carcinoma cells on woven PCL fabrics (φ = 0.5 to 12 μm) formed from a combination of electrospinning and wet spinning. Through the examination of cell attachment, proliferation and morphology, the authors in general concluded that electrospun fibrous scaffolds were cyto-compatible.

Although the motivation behind using nanofibrous scaffolds is to utilize the high surface-area-to-volume ratio of the fibers to enhance cell attachment, and also to mimic the ECM in order to control cellular functions and tissue regeneration, the majority of the research has been limited to analyzing only cellular attachment to the scaffold, sometimes producing contradicting results depending on the cell type and materials used. The exact benefits behind using nanofibrous scaffolds remain to be evaluated using more in-depth assessment of cellular functions. Nonetheless, studies available so far do illustrate the potential of electrospun fibrous meshes in tissue engineering applications.

5. Summary

Continuous nanofibers represent a novel class of nanomaterials with interesting potential for nanomedicine. Produced by a versatile and inexpensive electrospinning process, nanofibers offer a unique route to combine topographical, biochemical, and mechanical (compliance) cues to improve cell culture. The random or oriented nanofibrous structure may lead to revolutionary biomimetic coatings and scaffolds for tissue engineering. Advances in this field would require broad interdisciplinary effort. The fertile areas of investigation would include better theoretical understanding of the electrospinning process, improved process control, novel characterization approach to investigate the cell-nanofiber interactions, biofunctionalization with ligand immobilization or drug encapsulation, and judicious application for regenerative medicine.

Acknowledgements

This work was supported in part by the National Science Foundation (YD) and NIH (KWL, EB003447 and Division of Johns Hopkins in Singapore).

References

1. Abrams GA, Bentley E, Nealey PF, Murphy CJ. Electron microscopy of the canine corneal basement membranes. Cells Tissues Organs 2002;170(4):251–7. [PubMed: 11919413]
2. Abrams GA, Goodman SL, Nealey PF, Franco M, Murphy CJ. Nanoscale topography of the basement membrane underlying the corneal epithelium of the rhesus macaque. Cell Tissue Res 2000;299(1):39–46. [PubMed: 10654068]
3. Colvin VL. The potential environmental impact of engineered nanomaterials. Nature Biotechnology 2003;21:1166–1170.
4. Kipen HM, Laskin DL. Smaller is not always better: nanotechnology yields nanotoxicology. American Journal of Physiology-Lung Cellular and Medecular Physiology 2005;289(5):L696–L697.
5. Hongu, T.; Phillips, GO. New Fibers. 2nd. Cambridge, England: Woodhead Publishing Limited; 1997.
6. Dzenis Y. Nanomanufacturing of Continuous Polymer Nanofibers by Electrospinning: A Review. Progress in Polymer Science. 2005in preparation (Invited Review)
7. Larrondo L, Manley R. Electrostatic fiber spinning from polymer melts. Parts I-III. Polymer Science: Polymer Physics Edition 1981;19:909, 921, 933.
8. Fennessey SF, Farris RJ. Electrospinning: Mechanical behavior of twisted and drawn polyacrylonitrile nanofiber. Abstracts of Papers of the American Chemical Society 2004;228:U507–U507.
9. Loscertales IG, Barrero A, Márquez M, Spretz R, Velarde-Ortiz R, Larsen G. Electrically forced coaxial nanojets for one-step hollow nanofiber design. Journal of the American Chemical Society 2004;126:5376–5377. [PubMed: 15113206]
10. Kim K, Yu M, Zong XH, Chiu J, Fang DF, Seo YS, Hsiao BS, Chu B, Hadjiargyrou M. Control of degradation rate and hydrophilicity in electrospun non-woven poly(D,L-lactide) nanofiber scaffolds for biomedical applications. Biomaterials 2003;24(27):4977–4985. [PubMed: 14559011]
11. Dzenis Y, Wen YK. Continuous carbon nanofibers for nanofiber composites. MRS Proceedings 2001;702:47481.
12. Dzenis, Y.; Feng, Y.; Larsen, G.; Turner, J.; Zeng, X. Modeling-Based Nanomanufacturing of Novel Continuous Nanocrystalline Ceramic Nanofibers with Superior Mechanical Properties. in 2003 NSF Nanoscale Science and Engineering Conference; Arlington, VA. December 16-18; 2003.
13. Cloupeau M, Prunet-Foch B. Electrohydrodynamic spraying functioning modes: a critical review. Journal of Aerosol Science 1994;25:1021.
14. Ganan-Calvo AM. On the theory of electrodynamically driven capillary jets. Journal of Fluid Mechanics 1997;335:165.
15. Spivak AF, Dzenis YA. A Condition on the Existence of a Conductive Liquid Meniscus in an External Electric Field. Journal of Applied Mechanics 1999;66:1026–1028.
16. Spivak, AF.; Dzenis, Y.; Reneker, DH. In A hydrodynamic model of electrospinning of a charged dielectric viscous jet. NSF Design and Manufacturing Grantees Conference Proceedings; Seattle. January 1997;
17. Dzenis, YA.; Spivak, AF.; Reneker, DH. Electrospinning of polymer nanofibers. in 13th U.S. National Congress of Applied Mechanics; Gainesville, Florida. June 21-26; 1998.
18. Dzenis, YA.; Reneker, DH.; Spivak, AF.; Fong, H. Bending Instability of a Charged Viscoelastic Jet in Electrospinning: Experimental Observations and Analysis. in NSF DMII Grantees Conference Proceedings; Vancouver. 2000 Jan.
19. Shin YM, Hohman MM, Brenner MP, Rutledge GC. Electrospinning: A whipping fluid jet generates submicron polymer fibers. Applied Physics Letters 2001;78(8):1149–1151.
20. Yarin AL, Koombhongse S, Reneker DH. Bending instability in electrospinning of nanofibers. Journal of Applied Physics 2001;89(5):3018–3026.
21. Dzenis Y. Spinning continuous fibers for nanotechnology. Science 2004;304:1917–1919. [PubMed: 15218134]

22. Deitzel JM, Kleinmeyer J, Harris D, Tan NCB. The effect of processing variables on the morphology of electrospun nanofibers and textiles. Polymer 2001;42(1):261–272.

23. Gupta P, Elkins C, Long TE, Wilkes GL. Electrospinning of linear homopolymers of poly(methyl methacrylate): exploring relationships between fiber formation, viscosity, molecular weight and concentration in a good solvent. Polymer 2005;46(13):4799–4810.

24. Zong X, Kim K, Fang D, Ran S, Hsiao BS, Chu B. Structure and process relationship of electrospun bioadsorbable nanofiber membranes. Polymer 2002;43:4403–4412.

25. Fong H, Chun I, Reneker DH. Beaded nanofibers formed during electrospinning. Polymer 1999;40 (16):4585–4592.

26. Koombhongse S, Liu WX, Reneker DH. Flat polymer ribbons and other shapes by electrospinning. Journal of Polymer Science Part B-Polymer Physics 2001;39(21):2598–2606.

27. Bognitzki M, Czado W, Frese T, Schaper A, Hellwig M, Steinhart M, Greiner A, Wendorff JH. Nanostructured fibers *via* electrospinning. Advanced Materials 2001;13(1):70–72.

28. Hana SO, Sonb WK, Youkc JH, Leed TS, Park WH. Ultrafine porous fibers electrospun from cellulose triacetate. Materials Letters 2005;59:2998–3001.

29. Megelski S, Stephens JS, Chase DB, Rabolt JF. Micro- and nanostructured surface morphology on electrospun polymer fibers. Macromolecules 2002;35(22):8456–8466.

30. Shenoy SL, Bates WD, Frisch HL, Wnek GE. Role of chain entanglements on fiber formation during electrospinning of polymer solutions: good solvent, non-specific polymer-polymer interaction limit. Polymer 2005;46(10):3372–3384.

31. Buttafoco L, Kolkman NG, Poot AA, Dijkstra PJ, Vermes I, Feijen J. Electrospinning collagen and elastin for tissue engineering small diameter blood vessels. Journal of Controlled Release 2005;101 (13):322–324. [PubMed: 15719516]

32. Lyoo WS, Youk JH, Lee SW, Park WH. Preparation of porous ultra-fine poly(vinyl cinnamate) fibers. Materials Letters 2005;59(28):3558–3562.

33. Matthews JA, Wnek GE, Simpson DG, Bowlin GL. Electrospinning of collagen nanofibers. Biomacromolecules 2002;3(2):232–238. [PubMed: 11888306]

34. Dersch R, Liu T, Schaper AK, Greiner A, Wendorff JH. Electrospun nanofibers: internal structure and intrinsic orientation. Journal of Polymer Science: Part A: Polymer Chemistry 2003;41:545–553.

35. Jiang H, Fang D, Hsiao D, Chu B, Chen W. Preparation and characterization of ibuprofen-loaded poly(lactide-co-clycolide) / poly(ethylene glycol)- g - chitosan electrospun membranes. J Biomater Sci Polymer Edn 2004;15(3):279–296.

36. Katti DS, Robinson KW, Ko FK, Laurencin CT. Bioresorbable nanofiber-based systems for wound healing and drug delivery: optimization of fabrication parameters. J Biomed Mater Res Part B: Appl Biomater 2004;70B:286–296. [PubMed: 15264311]

37. Zeng J, Xu X, Chen X, Liang Q, Bian X, Yang X, Jing X. Biodegradable electrospun fibers for drug delivery. Journal of Controlled Release 2003;92:227–231. [PubMed: 14568403]

38. Verreck G, Chun I, Peeters J, Rosenblatt J, Brewster ME. Preparation and characterization of nanofibers containing amorphous drug dispersions generated by electrostatic spinning. Pharmaceutical Research 2003;20(5):810–817. [PubMed: 12751639]

39. Kim K, Luu YK, Chang C, Fang D, Hsiao BS, Chu B, Hadjiargyrou M. Incorporation and controlled release of a hydrophilic antibiotic using poly(lactide-co-glycolide)-based electrospun nanofibrous scaffolds. Journal of Controlled Release 2004;98:47–56. [PubMed: 15245888]

40. Kenawy ER, Bowlin GL, Mansfield K, Layman J, Simpson DG, Sanders EH, Wnek GE. Release of tetracycline hydrochloride from electrospun poly(ethylene-co-vinylacetate, poly(lactic acid), and a blend. Journal of Controlled Release 2002;81:57–64. [PubMed: 11992678]

41. Melaiye A, Sun Z, Hindi K, Milsted A, Ely D, Reneker DH, Tessier CA, Youngs WJ. Silver (I)-imidazole cyclophane gemdiol complexes encapsulated by electrospun tecophilic nanofibers: formation of nanosilver particles and antimicrobial activity. J Am Chem Soc 2005;127:2285–2291. [PubMed: 15713108]

42. Luu YK, Kim K, Hsiao BS, Chu B, Hadjiargyrou M. Development of a nanostructured DNA delivery scaffold via electrospinning of PLGA and PLA-PEG block copolymers. Journal of Controlled Release 2003;89:341–353. [PubMed: 12711456]

43. Zeng J, Aigner A, Czubayko F, Kissel T, Wendroff JH, Greiner A. Poly(vinyl alcohol) nanofibers by electrospinning as a protein delivery system and the retardation of enzyme release by additional polymer coatings. Biomacromolecules 2005;6(3):1484–1488. [PubMed: 15877368]
44. Chew SY, Wen J, Yim EKF, Leong KW. Sustained release of proteins from electrospun biodegradable fibers. Biomacromolecules 2005;6(4):2017–2024. [PubMed: 16004440]
45. Kwon IK, Matsuda T. Co-electrospun nanofibers fabrics of poly(ι-lactide-co-ε-caprolactone) with Type I collagen or heparin. Biomacromolecules 2005;6:2096–2105. [PubMed: 16004450]
46. Zong X, Li S, Chen E, Garlick B, Kim Ks, Fang D, Chiu J, Zimmerman T, Brathwaite C, Hsiao BS, Chu B. Prevention of postsurgery-induced abdominal adhesions by electrospun bioabsorbable nanofibrous poly(lactide-co-glycolide)-based membranes. Annals of Surgery 2004;240(5):910–915. [PubMed: 15492575]
47. Xu C, Inai R, Kotaki M, Ramakrishna S. Electrospun nanofiber fabrication as synthetic extracellular matrix and its potential for vascular tissue engineering. Tissue Engineering 2004;10(78):1160–1168. [PubMed: 15363172]
48. Venugopal J, Ma LL, Yong T, Ramakrishna S. *In vitro* study of smooth muscle cells on polycaprolactone and collagen nanofibrous matrices. Cell Biology International 2005;29:861–867. [PubMed: 16153863]
49. Stankus JJ, Guan J, Fujimoto K, Wagner WR. Microintegrating smooth muscle cells into a biodegradable elastomeric fiber matrix. Biomaterials. 2005
50. Stitzel JD, Pawlowski KJ, Wnek GE, Simpson DG, Bowlin GL. Arterial smooth muscle cell proliferation on a novel biomimicking, biodegradable vascular graft scaffold. Journal of biomaterials applications 2001;16:22–33. [PubMed: 11475356]
51. Stitzel J, Liu J, Lee SJ, Komura M, Berry J, Soker S, Lim G, Dyke MV, Czerw R, Yoo JJ, Atala A. Controlled fabrication of a biological vascular substitute. Biomaterials. 2005
52. Xu C, Yang F, Wang S, Ramakrishna S. *In vitro* study of human vascular endothelial cell function on materials with various surface roughness. J Biomed Mater Res A 2004;71(1):154–61. [PubMed: 15368265]
53. Kwon IK, Kidoaki S, Matsuda T. Electrospun nano- to microfiber fabrics made of biodegradable copolyesters: structural characteristics, mechanical properties and cell adhesion potential. Biomaterials 2005;26(18):3929–3939. [PubMed: 15626440]
54. He W, Ma Z, Yong T, Teo WE, Ramakrishna S. Fabrication of collagen-coated biodegradable polymer nanofiber mesh and its potential for endothelial cells growth. Biomaterials 2005;26:7606–7615. [PubMed: 16000219]
55. Ma ZW, Kotaki M, Yong T, He W, Ramakrishna S. Surface engineering of electrospun polyethylene terephthalate (PET) nanofibers towards development of a new material for blood vessel engineering. Biomaterials 2005;26(15):2527–2536. [PubMed: 15585255]
56. Zong X, Bien H, Chung CY, Yin L, Fang D, Hsiao BS, Chu B, Entcheva E. Electrospun fine-textured scaffolds for heart tissue constructs. Biomaterials 2005;26:5330–5338. [PubMed: 15814131]
57. Yang F, Murugan R, Wang S, Ramakrishna S. Electrospinning of nano/micro scale poly(L-lactic acid) aligned fibers and their potential in neural tissue engineering. Biomaterials 2005;26(15):2603–2610. [PubMed: 15585263]
58. Riboldi SA, Sampaolesi M, Neuenschwander P, Cossu G, Mantero S. Electrospun degradable polyesterurethane membranes: potential scaffolds for skeletal muscle tissue engineering. Biomaterials 2005;26(22):4606–4615. [PubMed: 15722130]
59. Fujihara K, Kotaki M, Ramakrishna S. Guided bone regeneration membrane made of polycaprolactone/calcium carbonate composite nano-fibers. Biomaterials 2005;26:4139–4147. [PubMed: 15664641]
60. Bhattarai N, Edmondson D, Veiseh O, Matsen FA, Zhang M. Electrospun chitosan-based nanofibers and their cellular compatibility. Biomaterials 2005;26:6176–6184. [PubMed: 15885770]
61. Badami AS, Kreke MR, Thompson MS, Riffle JS, Goldstein AS. Effect of fiber diameter on spreading, proliferation and differentiation of osteoblastic cells on electrospun poly(lactic acid) substrates. Biomaterials. 2005
62. Shields KJ, Beckman MJ, Bowlin GL, Wayne JS. Mechanical properties and cellular proliferation of electrospun collagen type II. Tissue Engineering 2004;10(910):1510–1516. [PubMed: 15588410]

63. Li WJ, Danielson KG, Alexander PG, Tuan RS. Biological response of chondrocytes cultured in three-dimensional nanofibers poly(ε-caprolactone) scaffolds. Journal of biomedical material research 2003;67A(4):1105–1114.
64. Li WJ, Laurencin CT, Caterson EJ, Tuan RS, Ko FK. Electrospun nanofibrous structure: a novel scaffold for tissue engineering. Journal of biomedical material research 2002;60(4):613–621.
65. Jin HJ, Chen J, Karageorgiou V, Altman GH, Kaplan DL. Human bone marrow stromal cell responses to electrospun silk fibroin mats. Biomaterials 2004;25:1039–1047. [PubMed: 14615169]
66. Li WJ, Tuli R, Okafor C, Derfoul A, Danielson KG, Hall DJ, Tuan RS. A three-dimensional nanofibrous scaffold for cartilage tissue engineering using human mesenchymal stem cells. Biomaterials 2005;26:599–609. [PubMed: 15282138]
67. Li WJ, Tuli R, Huang X, Laquerriere P, Tuan RS. Multilineage differentiation of human mesenchymal stem cells in a three-dimensional nanofibrous scaffold. Biomaterials 2005;26:5158–5166. [PubMed: 15792543]
68. Zhang Y, Ouyang H, Lim CT, Ramakrishna S, Huang ZM. Electrospinning of gelatin fibers and gelatin/PCL composite fibrous scaffolds. Journal of Biomedical materials Research Part B: Applied Biomaterials 2005;72B:156–165.
69. Min BM, Lee G, Kim SH, Nam YS, Lee TS, Park WH. Electrospinning of silk fibroin nanofibers and its effect on the adhesion and spreading of normal human keratinocytes and fibroblasts *in vitro*. Biomaterials 2004;25:1289–1297. [PubMed: 14643603]
70. Min BM, Jeong L, Nam YS, Kim JM, Kim JY, Park WH. Formation of silk fibroin matrices with different texture and its cellular response to normal human keratinocytes. International Journal of Biological Macromolecules 2004;34(5):281–288. [PubMed: 15556229]
71. Khil MS, Bhattarai SR, Kim HY, Kim SZ, Lee KH. Novel fabricated matrix via electrospinning for tissue engineering. Journal of Biomedical Material Research Part B: Applied Biomaterials 2005;72 (1):117–24.
72. Zong X, Ran S, Kim KS, Fang D, Hsiao BS, Chu B. Structure and morphology changes during *in vitro* degradation of electrospun poly(glycolide-co-lactide) nanofiber membrane. Biomacromolecules 2003;4:416–423. [PubMed: 12625740]
73. Inai R, Kotaki M, Ramakrishna S. Structure and properties of electrospun PLLA single nanofibres. Nanotechnology 2005;16(2):208–213.
74. Jun Z, Hou HQ, Schaper A, Wendorff JH, Greiner A. Poly-L-lactide nanofibers by electrospinning - Influence of solution viscosity and electrical conductivity on fiber diameter and fiber morphology. E-Polymers. 2003
75. Cha DI, Kim HY, Lee KH, Jung YC, Cho JW, Chun BC. Electrospun nonwovens of shape-memory polyurethane block co-polymers. Journal of Applied Polymer Science 2005;96(2):460–465.
76. Tan EPS, Ng SY, Lim CT. Tensile testing of a single ultrafine polymeric fiber. Biomaterials 2005;26 (13):1453–1456. [PubMed: 15522746]
77. Lee KH, Kim HY, Khil MS, Ra YM, Lee DR. Characterization of nano-structured poly(epsilon-caprolactone) nonwoven mats *via* electrospinning. Polymer 2003;44(4):1287–1294.
78. Kenawy ER, Layman JM, Watkins JR, Bowlin GL, Matthews JA, Simpson DG, Wnek GE. Electrospinning of poly(ethylene-co-vinyl alcohol) fibers. Biomaterials 2003;24:907–913. [PubMed: 12504511]
79. Sanders EH, Kloefkorn R, Bowlin GL, Simpson DG, Wnek GE. Two-phase electrospinning from a single electrified jet: micro-encapsulation of aqueous reservoirs in poly(ethylene-co-vinyl acetate) fibers. Macromolecules 2003;36(11):3803–3805.
80. DemiR MM, Yilgor I, Yilgor E, Erman B. Electrospinning of polyurethane fibers. Polymer 2002;43:3303–3309.
81. Kidoaki S, Kwon IK, Matusda T. Mesoscopic spatial designs of nano- and microfiber meshes for tissue-engineering matrix and scaffold based on newly devised multilayering and mixing electrospinning techniques. Biomaterials 2005;26:37–46. [PubMed: 15193879]
82. McKee MG, Park T, Unal S, Yilgor I, Long TE. Electrospinning of linear and highly branched segmented poly(urethane urea)s. Polymer 2005;46(7):2011–2015.

83. Lee CH, Shin HJ, Cho IH, Kang YM, Kim IA, Park KD, Shin JW. Nanofiber alignment and direction of mechanical strain affect the ECM production of human ACL fibroblast. Biomaterials 2005;26(11): 1261–1270. [PubMed: 15475056]
84. Smit E, Buttner U, Sanderson RD. Continuous yarns from electrospun fibers. Polymer 2005;46(8): 2419–2423.
85. Bhattarai N, Cha DI, Bhattarai SR, Khil MS, Kim HY. Biodegradable electrospun mat: Novel block copolymer of poly (p-dioxanone-co-L-lactide)-block-poly (ethylene glycol). Journal of Polymer Science Part B-Polymer Physics 2003;41(16):1955–1964.
86. Norris ID, Shaker MM, Ko FK, MacDiarmid AG. Electrostatic fabrication of ultrafine conducting fibers: polyaniline / polyethylene oxide blends. Synthetic Metals 2000;114:109–114.
87. Deitzel JM, Kleinmeyer JD, Hirvonen JK, Tan NCB. Controlled deposition of electrospun poly (ethylene oxide) fibers. Polymer 2001;42:8163–8170.
88. Wu LL, Yuan XY, Sheng J. Immobilization of cellulase in nanofibrous PVA membranes by electrospinning. Journal of Membrane Science 2005;250(12):167–173.
89. Yao L, Haas TW, Guiseppi-Elie A, Bowlin GL, Simpson DG, Wnek GE. Electrospinning and stabilization of fully hydrolyzed poly(vinyl alcohol) fibers. Chem Mater 2003;15:1860–1864.
90. Ding B, Kim HY, Lee SC, Shao CL, Lee DR, Park SJ, Kwag GB, Choi KJ. Preparation and characterization of a nanoscale poly(vinyl alcohol) fiber aggregate produced by an electrospinning method. Journal of Polymer Science: Part B: Polymer Physics 2002;40(13):1261–1268.
91. Kim SH, Kim SH, Nair S, Moore E. Reactive electrospinning of cross-linked poly(2-hydroxyethyl methacrylate) nanofibers and elastic properties of individual hydrogel nanofibers in aqueous solutions. Macromolecules 2005;38:3719–3723.
92. Tan ST, Wendorff JH, Pietzonka C, Jia ZH, Wang GQ. Biocompatible and biodegradable polymer nanofibers displaying superparamagnetic properties. ChemPhysChem 2005;6:1461–1465. [PubMed: 16007710]
93. Jia HF, Zhu GY, Vugrinovich B, Kataphinan W, Reneker DH, Wang P. Enzyme-carrying polymeric nanofibers prepared *via* electrospinning for use as unique biocatalysts. Biotechnology Progress 2002;18(5):1027–1032. [PubMed: 12363353]
94. Bini TB, Gao S, Tan TC, Wang S, Lim A, Hai LB, Ramakrishna S. Electrospun poly(L-lactide-co-glycolide) biodegradable polymer nanofibre tubes for preipheral nerve regeneration. Nanotechnology 2004;15:1459–1464.
95. Wnek G. Polymer nanofibers by electrospinning and applications in medicine. Abstracts of Papers of the American Chemical Society 2004;227:U498–U498.
96. Bhattarai SR, Bhattarai N, Yi HK, Hwang PH, Cha DI, Kim HY. Novel biodegradable electrospun membrane: scaffold for tissue engineering. Biomaterials 2004;25:2595–2602. [PubMed: 14751745]
97. Huang L, Nagapudi K, Apkarian RP, Chaikof EL. Engineered collagen-PEO nanofibers and fabrics. Journal of biomaterial science, Polymer Edition 2001;12(9):979–993.
98. Matthews JA, Boland ED, Wnek GE, Simpson DG, Bowlin GL. Electrospinning of collagen type II: a feasibility study. Journal of bioactive and compatible polymers 2003;18:125–134.
99. Buttafoco L, Kolkman NG, Engbers-Buijtenhuijs P, Poot AA, Dijkstra PJ, Vermes I, Feijen J. Electrospinning of collagen and elastin for tissue engineering applications. Biomaterials. 2005
100. Huang L, Apkarian RP, Chaikof EL. High-resolution analysis of engineered type I collagen nanofibers by electron microscopy. Scanning 2001;23(6):372–375. [PubMed: 11770932]
101. WneK GE, Carr ME, Simpson DG, Bowlin GL. Electrospinning of Nanofiber Fibrinogen Structures. Nano Letters 2003;3(2):213–216.
102. Min BM, Lee SW, Lim NJ, You Y, Lee TS, Kang PH, Park WH. Chitin and chitosan nanofibers: electrospinning of chitin and deacetylation of chitin nanofibers. Polymer 2004;45:7137–7142.
103. Duan B, Dong C, Yuan X, Yao K. Electrospinning of chitosan solutions in acetic acid with poly (ethylene oxide). J Biomater Sci Polymer Edn 2004;15(6):797–811.
104. Geng X, Kwon OH, Jang J. Electrospinning of chitosan dissolved in concentrated acetic acid solution. Biomaterials 2005;26:5427–5432. [PubMed: 15860199]
105. Stephens JS, Fahnestock SR, Farmer RS, Kiick KL, Chase DB, Rabolt JF. Effects of electrospinning and solution casting protocols on the secondary structure of a genetically engineered dragline spider

silk analogue investigated via fourier transform Raman spectroscopy. Biomacromolecules 2005;6 (3):1405–1413. [PubMed: 15877359]

106. Zarkoob S, Eby RK, Reneker DH, Hudson SD, Ertley D, Adams WW. Structure and morphology of electrospun silk nanofibers. Polymer 2004;45:3973–3977.
107. Ayutsede J, Gandhi M, Sukigara S, Micklus M, Chen HE, Ko F. Regeneration of Bombyx mori silk by electrospinning. Part 3: characterization of electrospun nonwoven mat. Polymer 2005;46(5): 1625–1634.
108. Jin HJ, Fridrkh SV, Rutledge GC, Kaplan D. Electrospinning Bombyx mori silk with poly(ethylene oxide). Biomacromolecules 2002;3:1233–1239. [PubMed: 12425660]
109. Ohgo K, Zhao CH, Kobayashi M, Asakura T. Preparation of non-woven nanofibers of Bombyx mori silk, Samia cynthia ricini silk and recombinant hybrid silk with electrospinning method. Polymer 2003;44(3):841–846.
110. Sukigara S, Gandhi M, Ayutsede J, Micklus M, Ko F. Regeneration of Bombyx mori silk by electrospinning - part 1: processing parameters and geometric properties. Polymer 2003;44(19): 5721–5727.
111. Buchko CJ, Chen LC, Shen Y, Martin DC. Processing and microstructural characterization of porous biocompatible protein polymer thin films. Polymer 1999;40(26):7397–7407.
112. Nagapudi K, Brinkman WT, Thomas BS, Park JO, Srinivasarao M, Wright E, Conticello VP, Chaikof EL. Viscoelastic and mechanical behavior of recombinant protein elastomers. Biomaterials 2005;26:4695–4706. [PubMed: 15763249]
113. Nagapudi K, Brinkman WT, Leisen JE, Huang L, McMillan RA, Apkarian RP, Conticello VP, Chaikof EL. Photomediated solid-state cross-linking of an elastin-mimetic recombinant protein polymer. Macromolecules 2002;35(5):1730–1737.
114. Huang L, McMillan RA, Apkarian RP, Pourdeyhimi B, Conticello VP, Chaikof EL. Generation of synthetic elastin-mimetic small diameter fibers and fiber networks. Macromolecules 2000;33(8): 2989–2997.
115. Woerdeman DL, Ye P, Shenoy S, Parnas RS, Wnek GE, Trofimova O. Electrospun fibers from wheat protein: investigation of the interplay between molecular structure and the fluid dynamics of the electrospinning process. Biomacromolecules 2005;6:707–712. [PubMed: 15762633]
116. Fang X, Reneker DH. DNA fibers by electrospinning. J Macromol Sci - Phys 1997;B36(2):169–173.
117. Um IC, Fang D, Hsiao BS, Okamoto A, Chu B. Electrospinning and electro-blowing of hyaluronic acid. Biomacromolecules 2004;5:1428–1436. [PubMed: 15244461]
118. Xie JB, Hsieh YL. Ultra-high surface fibrous membranes from electrospinning of natural proteins: casein and lipase enzyme. Journal of Materials Science 2003;38(10):2125–2133.
119. Stankus JJ, Guan JJ, Wagner WR. Fabrication of biodegradable elastomeric scaffolds with sub-micron morphologies. Journal of Biomedical Materials Research Part A 2004;70A(4):603–614. [PubMed: 15307165]

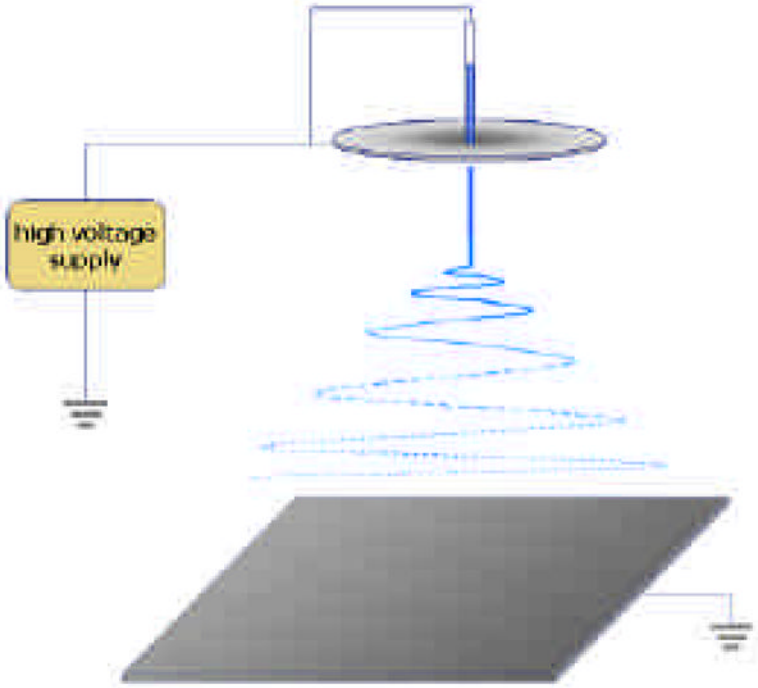

Fig. 1.
Schematic of electrospinning process.

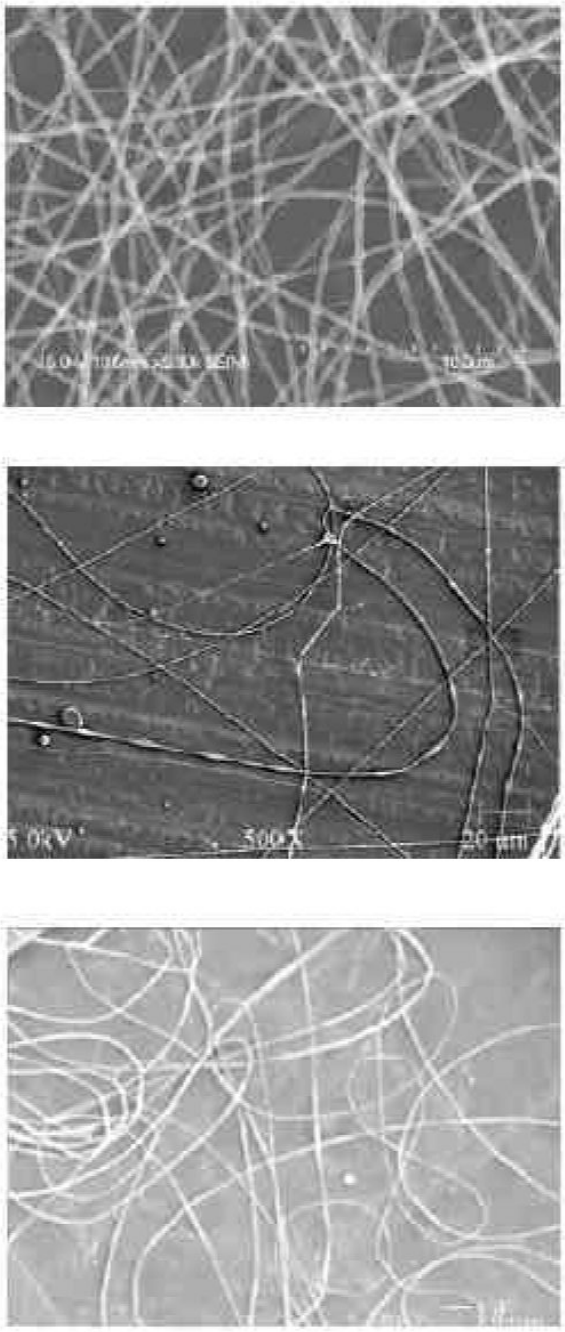

Fig. 2.
Examples of biocompatible PEO (a), biodegradable PLGA (b), and natural collagen (c) nanofibers produced by electrospinning.

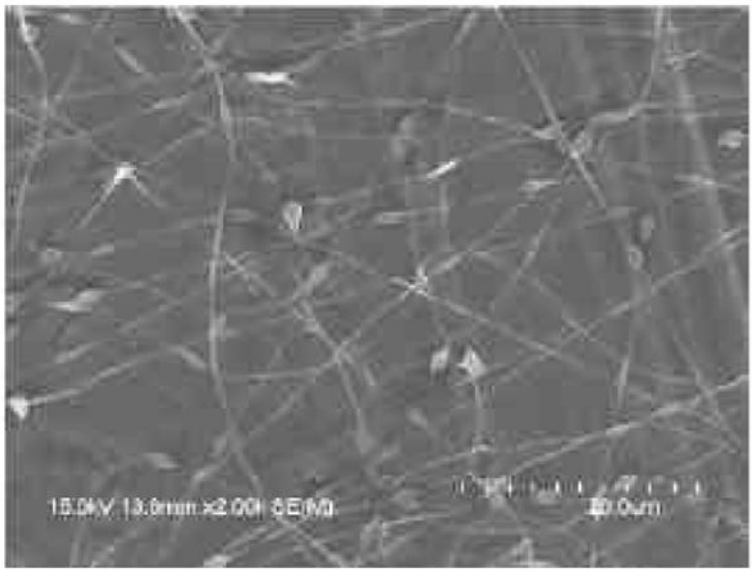

Fig. 3.
Example of beaded nanofibers as a result of varicose jet instability.

Fig. 4.
Electrospun collagen ribbons.

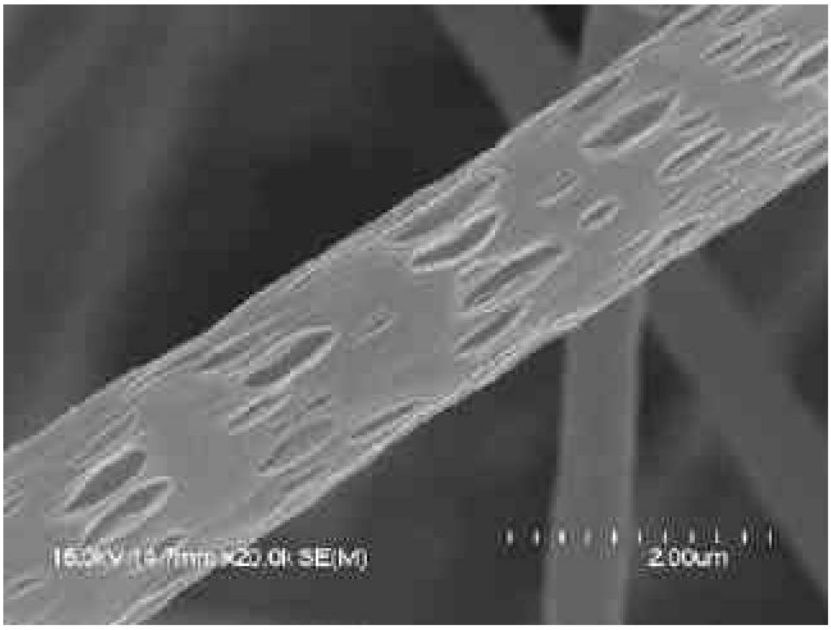

Fig. 5.
Porous biodegradable PLA fiber produced by electrospinning of solution in volatile solvent (dichloromethane).

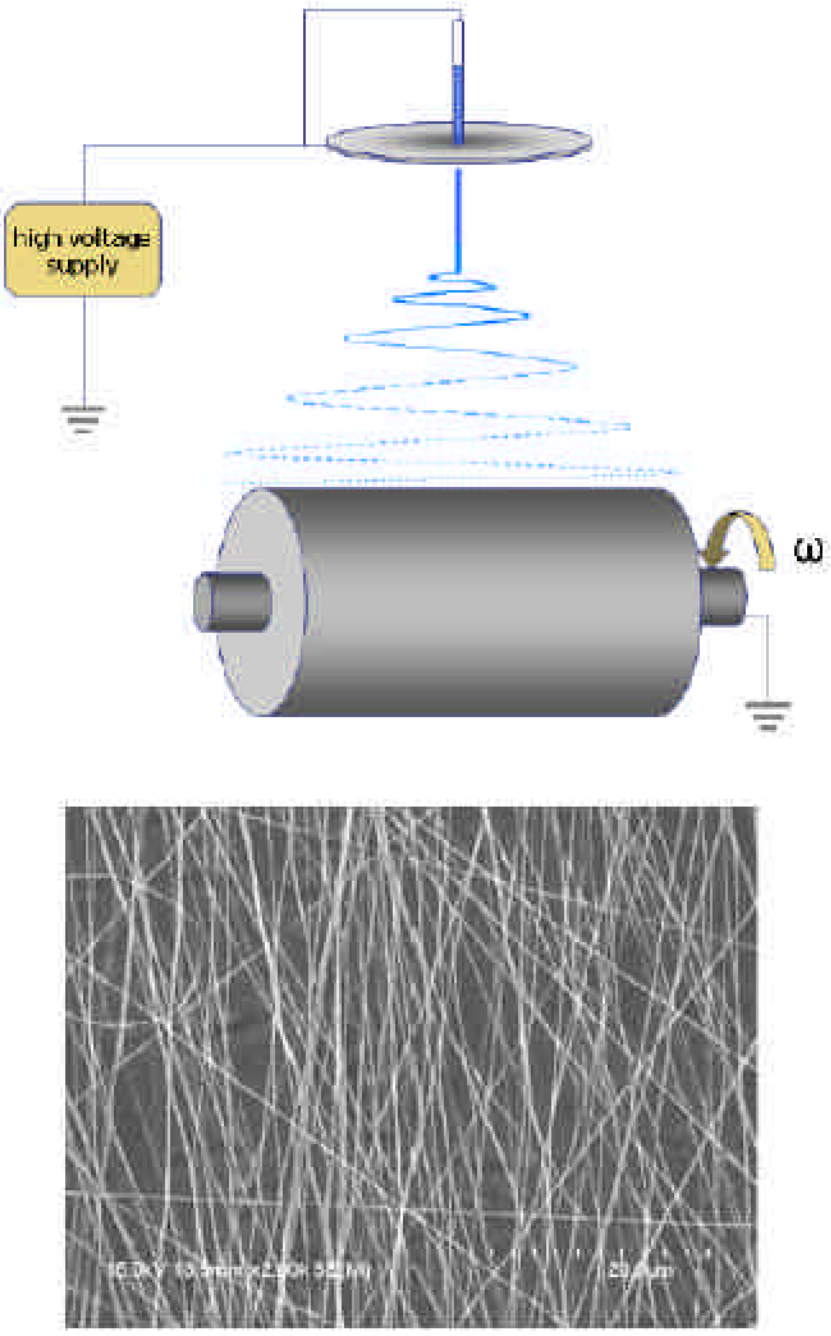

Fig. 6.
Schematic of conventional rotating drum for nanofiber collection and example of resulting partially aligned nanofiber sheet.

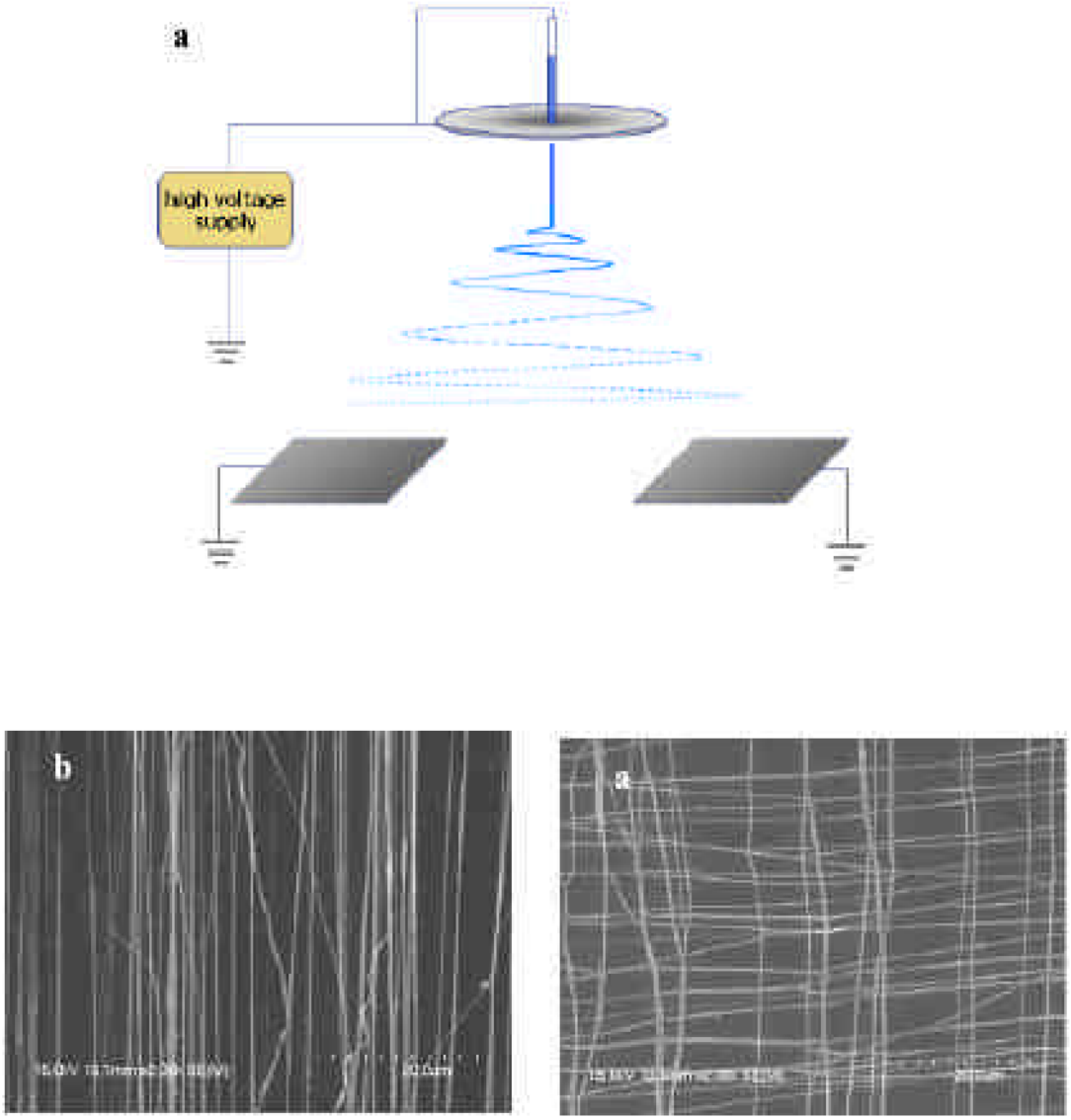

Fig. 7.
(a) Schematic of split electrode (gap) method of alignment and examples of unidirectional (b) and orthogonal (c) PEO nanofiber constructs produced by this method.

Table 1

Electrospun Biocompatible Materials

	Polymer	Processing	Size & Structure	Biodegradability	Biofunctionality
Synthetic	PLA [24,34,37, 40,50,52,53,56, 57,72-75]	**a.** Chloroform, 14w/v% **b.** DCM: DMF (70:30), 1-5wt% **c.** HFP, 10wt%; **d.** DMF, 30wt%; **e.** DCM, 1.5-4wt% **f.** DCM:MtOH (8:2), 7.5 & 12.5wt% **g.** DCM:Pyr (6:4), 7.5 & 12.5wt% **h.** DCM, 7.5wt% **i.** Water, 1 & 5wt% **j.** DCM, 4wt% **k.** DCM, 5wt% **l.** Chloroform, 0.1g/ml **m.** DCM:DMF (65:35), 6% **n.** DMF, 20-36wt% **o.** DCM:DMF (3:2), 20-36wt%	**a.** 10μm, R **b.** 235-3500nm, R/A **c.** 1μm, A **d.** 200-1000nm, R **e.** 0.34-1.35μm, R **f.** 610-890nm, R/A **g.** 610-890nm, R/A **h.** 610-890nm, R/A **i.** 50-300nm, R **j.** 4.5±0.34μm, R **k.** 800-2400nm, R **l.** 100-300nm, R **m.** 700-1000nm, R **n.** 200-1000nm, R **o.** 200-1000nm, R	Yes	• Drug encapsulation • Protein encapsulation • Magnetite nanoparticles encapsulation
	PCL [48,53,59, 61,63,66,67,71, 75-77]	**a.** THF:DMF (1:1), 0.14g/ml; **b.** Chloroform:MtOH (75:25), 7.5wt%, 10wt% **c.** DCM:DMF (100:0; 85:15; 75:25; 50:50; 40:60), 8-15wt% **d.** HFP, 7.4wt% **e.** DCM:Toluene (85:15;40:60), 10-15wt % **f.** DCM, 7.5wt%	**a.** 500-900 nm, R **b.** 600 ± 230nm, 150-500nm, 1.4±0.3μm, R/A **c.** 0.5-12μm, R **d.** 150-500nm, R/A **e.** 0.2-5.5μm, R **f.** 5.6±0.61μm, R	Yes	• CaCO3 • Protein adsorption
	PEVA [40,78, 79]	**a.** Chloroform, 14wt% **b.** 2-propanol:water (70:30), 2.5-20% w/v **c.** DCM, 13%	**a.** 10μm, R **b.** ~0.5-7μm, R **c.** 5-20μm, R	No	• Drug Encapsulation
	PET [55]	**a.** Trifluoroacetic acid, 0.2g/ml	**a.** 200-600nm, R	No	• Gelatin grafted
	PU [80-85]	**a.** DMF, 3.8-12.8wt% **b.** THF, 15wt% **c.** THF:IPA (1:2; 1:4), 10 & 10.8wt% **d.** DMF, 20% **e.** Melt **f.** THF:DMF (100:0; 70:30; 50:50; 30:70;0:100), 25%	**a.** ~60-800nm, R **b.** R **c.** R **d.** 500-800, R/A **e.** 5.8μm, R **f.** 250-400, R	No	

	Polymer	Processing	Size & Structure	Biodegradability	Biofunctionality
	PEO/PEG [81, 86,87]	**a.** Chloroform, 2-4wt% **b.** Water, 10wt% **c.** Chloroform, 1-4.5wt%	**a.** 0.95-2.1μm, R **b.** 270-400nm. R **c.** R	Yes	
	PVA [43,88-90]	**a.** Acetic acid buffer **b.** Water, 10wt% **c.** Water, 8-16wt% **d.** Water, 10wt%	**a.** 200nm, R **b.** 100-700nm, R **c.** 260-400nm, R **d.** 250-300, R	Yes	• Protein encapsulation
	pHEMA [91,92]	**a.** Monomer **b.** Water, 5wt%	**a.** 315 ± 140nm, R **b.** 150 – 300nm, R	No	• Protein encapsulation • Magnetite nanoparticles encapsulation
	PS [93]	**a.** MEK:DMF (1:1) in 0.5wt% LiCl, 8%	**a.** 120-1000nm, R		• Nitrophenyl ending groups on PS
	HPMC [38]	**a.** EtOH:MC (40:60), 12%	**a.** 300-500nm, R		• Drug encapsulation
Synthetic Co-polymers	PLGA [35,36, 39,42,46,47,64, 72,75,85,94]	**a.** THF:DMF (1:1),0.05g/ml **b.** HFP, 10wt% **c.** DMF, 30-35wt% **d.** THF:DMF (3:1), 0.2g/ml **e.** DMF, 37% **f.** HFP, 2-7wt% **g.** HFP, 7.5-15wt%	**a.** 500-800nm, R **b.** 1μm, R **c.** 0.25-5μm, R **d.** 0.34-1.5μm, R **e.** 500-1200nm, R **f.** 500-1000nm, R **g.** 400-1000, R/A	Yes	• Drug encapsulation
	PEG-PLA [39, 42,46,61,85]	**a.** DMF, 30-33wt% **b.** With PLGA (10,12,15%), DMF, 35% w/v **c.** HFP, 5-26t% **d.** DMF, 30-50wt%	**a.** R **b.** R **c.** 0.141-2.14μm, R **d.** 500-800nm, R	Yes	• Drug encapsulation • DNA encapsulation
	PCLEEP [44]	**a.** DCM, 12wt%	**a.** 0.46-5μm, A	Yes	• Protein encapsulation
	PLA – PCL [45, 47,53,54,95]	**a.** DCM, 4-11wt% **b.** HFP, 3wt% **c.** Acetone, 5wt% **d.** HFP, 3wt% **e.** DCM:DMF (wt ratio 70:30), 10wt% **f.** THF:acetone, 3-9wt% **g.** Acetone:Chloroform, 5wt%	**a.** 0.3-7μm, R **b.** 0.3-7μm, R **c.** 400-800nm, R **d.** R **e.** 470 ± 130nm, R **f.** 500-1500, R **g.** 200-800, A	Yes	• Glycosaminoglycan salt encapsulation • Protein adsorption
	PEUU [49]	**a.** HFP, 5 and 12wt%	a.	Yes	• Cell integration
	p(HEMA-co-MAA) [91]	**a.** Monomer	**a.** 315 ± 140nm, R	No	
	DegraPol [58]	**a.** Chloroform, 30wt%	**a.** 10μm, R	Yes	
	PPDO/PLLA-*b*-PEG [85,96]	**a.** DCM:DMF (100/0;75/25;40/60), 10-20%	**a.** 380-1400nm, R	Yes	

	Polymer	Processing	Size & Structure	Biodegradability	Biofunctionality
Natural	Collagen Type I, II and III [33,48, 62,81,97-100]	**a.** Type I:PEO (1:1) in 10mM HCl, 1-2wt % **b.** Type II, HFP, 0.04 & 0.1g/ml **c.** Type I/III, HFP, 0.083-0.06g/ml **d.** Type I, HFP, 1-7wt% **e.** Type II, HFP **f.** Type I (2% w/v): PEO (5% w/v) (1:1) in 10mM HCl with 42.5mM NaCl **g.** Type I, HFP, 75mg/ml **h.** 1wt% PEO in 10mg/ml Col I	**a.** 100-150nm, R **b.** 0.11-1.75μm, R **c.** 100-730nm, R **d.** 0.2-1.86μm, R **e.** 0.07-2.74μm, R **f.** 0.40 ± 0.05μm, R **g.** 300-375nm, R **h.** 50-150nm, R	Enzymatic	
	Gelatin [68]	**a.** Type A, TFE, 2.5-12.5 % w/v	**a.** R	Enzymatic	
	Fibrinogen [101]	**a.** HFP: 10X MEM (9:1), 0.083-0.167g/ml	**a.** 80 – 700nm, R	Enzymatic	
	Chitin & hitosan [60,102-104]	**a.** Chitin: HFP, 5wt% **b.** Chitosan:PEO (1:1,2:1,5:1), Acetic acid, 2-8wt% **c.** Chitosan (3%):PEO (3%) (60:40 to 90:10) in 0.5M acetic acid, 0-0.5wt% Triton X-100TM, 0-10wt% DMSO **d.** Chitosan: acetic acid (10-90%), 2.5-10wt%	**a.** 40-600nm, R **b.** 124 ±19nm, R **c.** 38-62nm, R / A **d.** 40-290nm, R	Enzymatic	
	Silk [65,69,70, 105-110]	**a.** Recombinant Dragline spider silk: HFP, 15wt% **b.** N. clavipes Dragline silk: HFP, 0.23 – 1.2wt% **c.** B. Mori silk: HFP 0.74wt% **d.** B. Mori silk: Formic acid, 9-15wt% **e.** B. Mori silk: PEO: Water, 4.8-8.8wt% **f.** B. Mori silk: HFP, 1.5wt% **g.** B. Mori silk: PEO (8:2) in water, 7.5wt % **h.** Formic acid, 8wt% **i.** Formic acid, 12wt% **j.** B. Mori silk, Formic acid, 9-15wt% **k.** B. Mori, Samia cynthia ricini, HFA, “2-10wt% **l.** B. Mori silk, Formic acid, 5-20%	**a.** 300nm, R **b.** 8-200nm, R **c.** 6.5-100nm, R **d.** 8-397nm, R **e.** 700-880nm, R **f.** R **g.** 700 ± 50nm, R **h.** 80nm, R **i.** 80nm, R **j.** 8-397nm, R **k.** 100-1000nm, R **l.** 12-1500nm, R	Enzymatic	• Protein adsorption
	Silk mimetic peptide [111]	**a.** Formic acid, 0.8-16.2wt%	**a.** 200-2000, R	Enzymatic	
	Elastin [99]	**a.** Elastin (5wt%): PEO (1%w/v) (5:1) in 10mM HCl, 42.5mM NaCl	**a.** 0.5μm, R	Enzymatic	

	Polymer	Processing	Size & Structure	Biodegradability	Biofunctionality
	Elastin mimetic peptides [112-114]	**a.** TFE, 10wt% **b.** Water, 10wt% **c.** Water, 10-15wt% **d.** Water, 5-20wt%	**a.** 100-400nm, R **b.** 0.8-3μm, R **c.** 300-1500, R **d.** 200-3000nm, R	Enzymatic	
	Wheat protein [115]	**a.** HFP, 5 & 10% w/v	**a.** 100-5μm, R	Enzymatic	
	DNA [116]	**a.** Water:EtOH (70:30)	**a.** >30nm, R	Enzymatic	
	Hyaluronic Acid [117]	**a.** aq. HCl (pH=1.5), 1.3-2.5 w/v%	**a.** 10s of nm, R	Enzymatic	
	Cellulose acetate [1,34]	**a.** Acetone: DMAc (2:1), 15% **b.** Acetone: DMAc (2:1), 12.5-20%	**a.** 100-450nm, R **b.** 100-1000nm, R	Enzymatic	
	Casein [118]	**a.** Triethanolamine with PEO or PVA, 5-10%	**a.** 100-500nm, R	Enzymatic	
Synthetic / Natural polymer blends	Collagen Type I, Elastin & PLGA [51]	**a.** Col: Elastin: PLGA (wt ratio 45:15:40) in HFP, 15 w/v%	**a.** 0.720 ± 0.35μm, R	Yes; Enzymatic	
	Collgen Type I, Elastin & PEO [99]	**a.** Col: Elastin (3:1, 2:1, 1:2, 1:3) in 10mM HCl, 1-5% w/v; PEO (0.5wt%) in 10mM HCl; 42.5mM NaCl	**a.** 220-600nm, R	Enzymatic	
	Gelatin, PCL [68]	**a.** 10% w/v gelatin/TFE:10% w/v PCL/ TFE '(50:50)	**a.** ~1μm, R	Yes; Enzymatic	
	Collagen Type I, PLCL [45]	**a.** Col: PLCL (0-100%) in HFP, 3wt%	**a.** 120-520nm, R	Yes; Enzymatic	
	Styrenated gelatin [81]	**a.** HFP, 1-10wt%	**a.** 200-2000nm, R	No	
	PEUU/Collagen Type I [119]	**a.** PEUU:Col (2.5-90wt%); HFP, 5wt%	**a.** 100-900nm, R	Enzymatic	

A: Aligned, non-woven mesh; DCM: Dichloromethane; DegraPol: polyesterurethane with poly((R)-3-hydroxybutyric acid)-diol and poly(caprolactone-co-glycolide)-diol; DMAc: Dimethylacetamide; DMF: Dimethylformamide; DMSO: Dimethylsulphoxide; AIBN: 2,2′-azobis(isobutyronitrile); EGDMA: ethylene glycol-dimethacrylate; EtOH: Ethanol; HEMA: 2, hydroxyethyl methacrylate; HFA: hexafluoroacetone; HFP: 1,1,1,3,3,3 hexafluoro-2-propanol; HPMC: hydroxypropyl methylcellulose; IPA: isopropyl alcohol; MAA: methacrylic acid; MC: Methyl chloride; MEM: minimal essential medium; MtOH: Methanol; PCL: poly(caprolactone); PCLEEP: poly(caprolactone-co-ethyl ethylene phosphate); PEG: poly(ethylene glycol); PEO: poly(ethylene oxide); PET: poly(ethylene terephthalate); PEVA: poly(ethylene-co-vinyl acetate); PLA: poly(lactic acid); PLGA: poly(lactic-co-glycolic acid); PS: poly(styrene); PU poly(urethane); PVA poly(vinyl alcohol); Pyr: Pyridine; R: Random, non-woven mesh; TFE: 2,2,2 Trifluoroethanol; THF: Tetrahydrofuran.